

1 **Biosynthesis of the Dihydrochalcone Sweetener Trilobatin Requires *Phloretin***
2 ***Glycosyltransferase 2***

3

4 Yule Wang ^{a*}, Yar-Khing Yauk ^{b*}, Qian Zhao ^a, Cyril Hamiaux ^b, Zhengcao Xiao ^a,
5 Kularajathevan Gunaseelan ^b, Lei Zhang ^a, Sumathi Tomes ^b, Elena López-Girona ^c, Janine
6 Cooney ^d, Houhua Li ^e, David Chagné ^c, Fengwang Ma ^a, Pengmin Li ^{a+}, Ross G. Atkinson ^b

7

8 ^a State Key Laboratory of Crop Stress Biology for Arid Areas/Shaanxi Key Laboratory of
9 Apple, College of Horticulture, Northwest A&F University, Yangling, Shaanxi 712100, China

10 ^b The New Zealand Institute for Plant and Food Research Ltd (PFR), Private Bag 92169,
11 Auckland, New Zealand

12 ^c PFR, Private Bag 11600, Palmerston North 4442, New Zealand

13 ^d PFR, Private Bag 3123, Hamilton 3240, New Zealand

14 ^e College of Landscape Architecture and Arts, Northwest A&F University, Yangling, Shaanxi
15 712100, China

16

17 * These authors contributed equally to the work

18 + Corresponding author: Pengmin Li

19 College of Horticulture, Northwest A&F University, Yangling 712100, Shaanxi, P.R. China

20 Telephone: +86 187 2924 2835

21 Email: lipm@nwafu.edu.cn

22

23 **Short title**

24 *PGT2* is Required for Trilobatin Biosynthesis

25

26 **One sentence summary**

27 Genetic, biochemical and molecular characterization of *phloretin glycosyltransferase 2* reveals
28 its importance to the production of sweet-tasting trilobatin (phloretin-4'-*O*-glucoside) in wild
29 apple.

30

31 **Keywords:** apple, dihydrochalcone, glucoside, glycosyltransferase, *Malus*, phloretin,

32 sweetener, trilobatin

33

34 **FOOTNOTES**

35

36 **AUTHOR CONTRIBUTIONS**

37 Y.W., Y.Y., F.M., H.L., R.A., and P.L. designed the research; R.A. and P.L. ran the sensory
38 evaluation; Y.W.; Q.Z., and S.T. produced the transgenic plants; E.L.G., K.G. and D.C.
39 performed the mapping and HRM analysis; J.C. and Z.X. conducted LC-MS and HPLC
40 analyses; C.H. did the structural analysis; Y.W., Q.Z. and L.Z. undertook the protein
41 purification; Y.W. and Y.Y. carried out transcriptomic, HPLC, biochemical and molecular
42 analyses; Y.W., P.L. and R.A. analyzed data and wrote the paper.

43

44 **ORCID NUMBERS**

45 YW: 0000-0001-9932-124X; YY: 0000-0003-4744-6002; QZ: 0000-0002-8716-8193; CH:
46 0000-0001-9198-3441; ZX: 0000-0003-1336-5749; KG: 0000-0001-9009-0334; LZ:
47 0000-0003-3290-6678; ST: 0000-0001-7704-5432; EL-G: 0000-0003-0376-6135; JC:
48 0000-0002-2547-0100; HL: 0000-0002-3550-081X; DC: 0000-0003-4018-0694; FM:
49 0000-0003-0608-2521; RA: 0000-0002-7062-6952 ; PL: 0000-0003-3514-0153

50

51 **FUNDING**

52 This work was funded by the National Key R&D Program of China (2018YFD1000200) and
53 the New Zealand Ministry of Business, Innovation and Employment and internal PFR funding
54 derived in part from apple variety and royalty income.

55

56 YW's visit to PFR was supported by the Innovation Capability Support Plan (2018GHJD-11)
57 and the Key Research & Development Program (S2019-YF-GHMS-0050) of Shaanxi
58 Province, China.

59

60 **CORRESPONDING AUTHOR:**

61 Pengmin Li email: Email: lipm@nwafu.edu.cn

62

63 **ABSTRACT**

64 Epidemics of obesity and type 2 diabetes drive strong consumer interest in plant-based low
65 calorie sweeteners. Trilobatin (phloretin-4'-*O*-glucoside) is a sweetener found at high
66 concentrations in the leaves of a range of crabapple (*Malus*) species, but not in domesticated
67 apple (*M. × domestica*) leaves, which contain trilobatin's bitter positional isomer phloridzin
68 (phloretin-2'-*O*-glucoside). Variation in trilobatin content was mapped to the *Trilobatin* locus
69 on linkage group 7 in a segregating population developed from a cross between domesticated
70 apples and crabapples. *Phloretin glycosyltransferase 2 (PGT2)* was identified by
71 activity-directed protein purification and differential gene expression analysis in samples high
72 in trilobatin but low in phloridzin. Markers developed for *PGT2* co-segregated strictly with
73 the *Trilobatin* locus. Biochemical analysis showed *PGT2* efficiently catalyzed
74 4'-*O*-glycosylation of phloretin to trilobatin as well as 3-hydroxyphloretin to sieboldin
75 (3-hydroxyphloretin-4'-*O*-glucoside). Transient expression of *MdDBR* (double bond
76 reductase), *MdCHS* (chalcone synthase) and *PGT2* genes reconstituted the apple pathway for
77 trilobatin production in *Nicotiana benthamiana*. Transgenic *M. × domestica* plants
78 over-expressing *PGT2* produced high concentrations of trilobatin in young leaves. Transgenic
79 plants were phenotypically normal, and no differences in disease susceptibility were observed
80 compared to wildtype plants grown under simulated field conditions. Sensory analysis
81 indicated that apple leaf teas from *PGT2* transgenics were readily discriminated from control
82 leaf teas and were perceived as significantly sweeter. Identification of *PGT2* allows
83 marker-aided selection to be developed to breed apples containing trilobatin, and for high
84 amounts of this natural low calorie sweetener to be produced via biopharming and metabolic
85 engineering in yeast.

86 **INTRODUCTION**

87 Diabetes is a major public health problem that is approaching epidemic proportions
88 globally. The key risk factor linked with type 2 (adult-onset) diabetes is obesity, which is
89 associated with physical inactivity and over-eating (Bray and Popkin, 2014). One response to
90 this health crisis by the food and beverage industry has been to develop products utilizing a
91 range of non-sugar sweeteners to reduce calorie intake. Artificial sweeteners such as
92 aspartame, sucralose and saccharin are the most widely used (Kroger et al., 2006); however,
93 there has been increasing consumer awareness and demand for the use of natural low calorie
94 sweeteners. Natural compounds with intense sweetening capacity can be found in numerous
95 chemical families, including proteins, terpenoids and flavonoids. Examples of plant-based
96 sweeteners include steviol glycosides from stevia (*Stevia rebaudiana*) leaves, mogrosides
97 from the juice of monkfruit (*Siraitia grosvenorii*), and glycyrrhizin from liquorice
98 (*Glycyrrhiza glabra*) roots (Kim and Kinghorn, 2002).

99 Trilobatin is a plant-based sweetener that is reported to be ~100x sweeter than sucrose (Jia
100 et al., 2008). It is found at high concentrations in the leaves of a range of crabapple species,
101 including *Malus trilobata*, *M. sieboldii* and *M. toringo* (Williams, 1982; Gutierrez et al.,
102 2018b). It is not found in the domesticated apple (*M. × domestica*), but has been reported in
103 low amounts in the leaves of wild grape (*Vitis*) species (Tanaka et al., 1983). Some
104 *Lithocarpus* species also contain trilobatin and their leaves are used to prepare sweet tea in
105 China (Sun et al., 2015). The potential utility of trilobatin as a sweetener is recognized in
106 many food and beverage formulations e.g. (Jia et al., 2008; Walton et al., 2015); however, its
107 usefulness is limited by its scarcity. Methods for extraction have been documented from a
108 range of tissues (Sun, 2015; Sun and Zhang, 2015) and following biotransformation of citrus
109 waste (Lei et al., 2018). Biosynthesis of trilobatin in yeast has also been achieved
110 (Eichenberger et al., 2016), but efficient production has been hampered by lack of knowledge
111 of all the enzymes in the biosynthetic pathway.

112 Sweet-tasting trilobatin (phloretin-4'-*O*-glucoside) and bitter-tasting phloridzin
113 (phloretin-2'-*O*-glucoside) are positional isomers of the dihydrochalcone (DHC) phloretin,
114 which is produced on a side branch of the phenylpropanoid pathway. The first committed step
115 in the biosynthesis of DHCs can be catalyzed by a double bond reductase (DBR) that converts

116 *p*-coumaryl-CoA to *p*-dihydrocoumaryl-CoA (Gosch et al., 2009; Dare et al., 2013b; Ibdah et
117 al., 2014). The next step involves decarboxylative condensation and cyclisation of
118 *p*-dihydrocoumaryl-CoA and three units of malonyl-CoA by chalcone synthase (CHS) to
119 produce phloretin (Gosch et al., 2009; Yahyaa et al., 2017). The final step in the pathway
120 requires the action of UDP-glycosyltransferases (UGTs) to attach glucose at either the 2' or 4'
121 positions of the chalcone A-ring. Another apple DHC, sieboldin
122 (3-hydroxyphloretin-4'-*O*-glucoside), is also glycosylated at the 4' position either after the
123 conversion of phloretin to hydroxyphloretin or by conversion of trilobatin directly to
124 sieboldin.

125 UGTs are typically encoded by large gene families, with over 100 genes having been
126 described in *Arabidopsis* (Ross et al., 2001) and over 200 genes in the *M. × domestica*
127 genome (Caputi et al., 2012). All UGTs contain a conserved Plant Secondary Product
128 Glycosyltransferase (PSPG) motif that binds the UDP moiety of the activated sugar (Li et al.,
129 2001). Although some UGTs can utilize a broad range of acceptor substrates (Yauk et al.,
130 2014; Hsu et al., 2017), others have been shown to be highly specific (Fukuchi-Mizutani et
131 al., 2003; Jugdé et al., 2008). Systematic classification can facilitate the identification of
132 some UGT activities; however, functionality is generally difficult to ascribe through
133 phylogenetic relatedness alone. In apple, multiple UGTs have been identified that catalyze the
134 2'-*O*-glycosylation of phloretin to phloridzin: UGT88F1/*MdPGT1* (Jugdé et al., 2008),
135 UGT88F8 (Elejalde-Palmett et al., 2018), UGT88F4, UGT71K1 (Gosch et al., 2010), and
136 UGT71A15 (Gosch et al., 2012).

137 Dihydrochalcone levels have been manipulated in transgenic apples by down-regulation or
138 over-expression of UGTs and other genes in the phenylpropanoid pathway. UGT88F1
139 knockdown lines showed significantly reduced phloridzin accumulation (30% of wildtype)
140 and were severely dwarfed, with greatly reduced internode lengths and narrow lanceolate
141 leaves (Dare et al., 2017). UGT88F1 knockdown lines also showed increased resistance to
142 *Valsa* canker infection (Zhou et al., 2019). *MdCHS* knockout lines with 3-5% of wildtype
143 foliar phloridzin levels also showed a severely dwarfed growth pattern (Dare et al., 2013b).
144 Overexpression of UGT71A15 in transgenic apples increased the molar ratio of phloridzin to
145 phloretin, but did not affect plant morphology or susceptibility to the fire blight causing

146 bacterium *Erwinia amylovora* (Gosch et al., 2012). Overexpression of a chalcone
147 3'-hydroxylase in transgenic apple seedlings increased concentrations of 3-hydroxyphloridzin
148 and reduced susceptibility to both fire blight and apple scab (Hutabarat et al., 2016).

149 Two apple enzymes, UGT71A15 and UGT75L17 (*MdPh-4'-OGT*), that glycosylate
150 phloretin at the 4' position *in vitro* have been reported (Gosch et al., 2012; Yahyaa et al.,
151 2016). However, these proteins are expressed in the leaves and fruit of domesticated apples,
152 which do not accumulate trilobatin. To identify the glycosyltransferase leading to the
153 production of trilobatin in planta, we focused on tissue from a range of wild apple accessions
154 that produced trilobatin and sieboldin, and compared this with material from cultivated and
155 wild apples producing only phloridzin. Using a range of genetic, biochemical, molecular and
156 transgenic tools, we demonstrate that *phloretin glycosyltransferase 2 (PGT2)* is responsible
157 for trilobatin production in *Malus*, and that its over-expression increases perception of
158 sweetness in apple leaf teas.

159 RESULTS**160 Candidate Glycosyltransferases Identified by Activity-directed Protein Purification**

161 Tissues high in phloretin 4'-oGT (Ph4'-oGT) activity required for trilobatin production, but
162 containing very low phloretin 2'-oGT (Ph2'-oGT) activity for phloridzin synthesis, were used
163 to identify candidate Ph4'-oGTs by activity-directed protein purification. Flower petals of the
164 crabapple hybrid 'Adams' were identified as suitable experimental material as they have low
165 amounts of Rubisco compared with leaves, but higher Ph4'-oGT activity compared with fruit.
166 Purification involved sequential chromatographic steps (Q-sepharose, phenyl sepharose and
167 Superdex 75; Figure 1A–C), after which fractions with high Ph4'-oGT activity were pooled
168 and used for further purification. In the final step, after size exclusion chromatography, four
169 protein fractions with different Ph4'-oGT enzyme activities were analyzed by SDS-PAGE.
170 The abundance of a single band 44–66 kDa (the size expected of a typical UGT) changed in a
171 similar pattern (Figure 1D) to that of the Ph4'-oGT activities (Figure 1C). This band was
172 subjected to LC-MS/MS analysis and peptides corresponding to 50 proteins were identified in
173 the *M. × domestica* 'Golden Delicious' v1.0 genome assembly (Velasco et al., 2010) (Table
174 S1). Of the five most abundant proteins, peptides corresponding to gene models
175 MDP0000836043/MDP0000318032, encoding predicted UDP-glycosyltransferase 88A1-like
176 proteins, were observed at highest abundance (26% of total peptides) (Table 1).

177

178 Candidate Glycosyltransferases Identified by Differential Gene Expression Analysis

179 A second approach using differential gene expression (DGE) analysis was used to identify
180 candidate Ph4'-oGTs in tissues high in trilobatin but low in phloridzin. A cross was produced
181 between the ornamental crabapple hybrid 'Radiant' (containing both trilobatin and phloridzin),
182 and *M. × domestica* 'Fuji' (containing only phloridzin). The F1 progeny were separated into
183 two phenotypes with or without trilobatin for RNA extraction and transcriptome analysis.
184 Expression levels of 109 genes were up-regulated at least 16-fold (log₂-fold change >4) in
185 progeny producing trilobatin (Table S2). Of the five genes showing the greatest log-fold
186 change, the expression level of the predicted UDP-glycosyltransferase 88A1-like protein
187 MDP0000836043 exhibited the largest differential expression, and was up-regulated over
188 128-fold (log₂-fold change >7) in plants with trilobatin compared with those without (Table

189 2).

190

191 **Mapping Concentrations of Trilobatin and Candidate genes in a Segregating Population**

192 Trilobatin levels were mapped in a segregating population developed from a cross between
193 domesticated and wild apples ('Royal Gala' x Y3). The female parent 'Royal Gala' (*M. ×*
194 *domestica*) produced only phloridzin, whilst the male parent Y3 (derived from *M. sieboldii*)
195 produced both trilobatin and phloridzin. Of the fifty-one plants phenotyped, 30 contained
196 trilobatin and phloridzin, and 21 phloridzin alone. The segregation ratio (1:0.7; $\chi^2 = 1.59$)
197 suggested trilobatin content was segregating as a qualitative trait controlled by a single gene.
198 Data obtained by screening leaf DNA with the International RosBREED SNP Consortium
199 (IRSC) 8K SNP array (Chagné et al., 2012) were analyzed using JoinMap version 4.0 (van
200 Ooijen, 2006). A single locus for control of trilobatin biosynthesis (*Trilobatin*) was identified
201 on the lower arm of linkage group (LG)7, distal to a single nucleotide polymorphism (SNP)
202 marker located at position 32,527,873 bp (Figure 2A) on the 'Golden Delicious'
203 doubled-haploid genome assembly (GDDH13 v1.1) (Daccord et al., 2017). The locus was
204 further defined using high resolution melting (HRM) SNP markers developed from two
205 candidate *PGT* genes at 34,460,000–34,461,000 bp (Figure 2A, B) close to the base of LG7
206 (total length of LG7 is 36,691,129 in GDDH13 v1.1). The position mapped on LG7 was
207 consistent with one of the three independently segregating loci for DHC content reported
208 recently in *Malus*, using linkage and association analysis (Gutierrez et al., 2018a).

209 Genetic mapping by HRM marker analysis of gene model MDP0000836043, the candidate
210 UDP-glycosyltransferase 88A1-like protein identified by activity-directed protein purification
211 and DEG analysis, demonstrates that it co-locates with the locus identified for trilobatin
212 production on LG7 (Figure 2A). In the 'Golden Delicious' v1.0p assembly (Velasco et al.,
213 2010) MDP0000836043 is located at ~24,531,751 bp and corresponds to gene models
214 MD07G1281000/1100 (located at 34,459,260 bp) in the doubled-haploid assembly GDDH13
215 v1.1 (Figure 2B). The second UDP-glycosyltransferase 88A1-like protein identified by
216 activity-directed protein purification encoded by MDP0000318032 (MD07G1280800) is
217 located ~10.3 kb away in both assemblies (Figure 2B). Four SNP variants identified in the
218 region of these two UDP-glycosyltransferase gene models were used to develop markers for

219 HRM analysis (Figure S1, HRM primer sequences in Table S3). The mapping results
220 validated the position of the MDP0000836043 and MDP0000318032 on LG7 (Figure 2A),
221 and three of the markers (HRM1–3) showed precise concordance with presence/absence of
222 trilobatin in the segregating progeny (Table S4). HRM1 and 3 amplified both
223 MDP0000836043 (MD07G1281000/1100) and MDP0000318032 (MD07G1280800), whilst
224 HRM2 was specific for MDP0000836043 (MD07G1281000/1100). HRM4 was not specific to
225 the locus and was not used further.

226

227 **Biochemical Characterization of *PGT2* and *PGT3***

228 Complete open reading frames (ORFs) corresponding to MDP0000836043 (hereafter
229 termed *PGT2*, UGT88A32) were amplified from the leaves of six *Malus* accessions. The
230 *PGT2* ORFs from five accessions synthesizing trilobatin showed 91–94% amino acid identity
231 to the MDP0000836043 gene model from *M. domestica* ‘Golden Delicious’ (Figure S2). A
232 complete ORF for *PGT2* obtained from the leaves of *M. domestica* ‘Fuji’ was identical to that
233 obtained from *M. toringoides*, although *PGT2* was difficult to obtain from ‘Fuji’ because of
234 very low expression levels. The complete ORF corresponding to MDP0000318032 (termed
235 *PGT3*, UGT88A33) was also amplified from five *Malus* accessions and exhibited 97–99%
236 identity to the MDP0000318032 gene model from ‘Golden Delicious’, and 85–87% identity
237 to *PGT2* (Figure S3).

238 *PGT2* and *PGT3* from five *Malus* accessions and *PGT1* from ‘Fuji’ were expressed in
239 *Escherichia coli* and the products formed using phloretin and UDP-glucoside as substrates
240 were determined by HPLC. All purified recombinant *PGT2* enzymes produced a single peak
241 at 7.5 min that ran at the same retention time as the trilobatin standard (Figure 3A). A
242 representative HPLC trace for the product produced by *PGT2* from *M. toringoides* is shown in
243 Figure 3B. All purified recombinant *PGT3* enzymes (Figure 3C) and *PGT1* from ‘Fuji’
244 (Figure 3D) produced a peak at 6.0 min with the same retention time as phloridzin (Figure
245 3A), but no peak for trilobatin. No phloridzin or trilobatin were produced by the empty vector
246 control (Figure 3E).

247 The substrate specificity of recombinant *PGT2* from *M. toringoides* was further
248 characterized using UDP-glucoside as the sugar donor and twelve substrates typically found

249 in apple or with structural homology to phloretin (Table 3). The products of each reaction
250 were determined by LC-MS/MS. Phloretin was the best acceptor for PGT2 and base peak
251 plots indicated that a single peak at 21.5 min was formed that co-eluted with the trilobatin
252 standard (Figure 4A, B). PGT2 also catalyzed glycosylation of 3-OH phloretin to produce
253 sieboldin (Figure 4C, D) with a relatively high conversion rate of ~60% (Table 3).
254 Quercetin-3-*O*-glucoside was detected as a reaction product using quercetin (Figure S4A–F)
255 with a lower conversion rate of 9.1% (Table 3). This result is surprising, as the 4' position of
256 dihydrochalcones corresponds to the 7 position of quercetin, but no quercetin-7-*O*-glucoside
257 was observed. No products were detected in reactions with the other acceptor substrates,
258 however trace activity (1.4% compared with UDP-glucose) was detected with *PGT2* using
259 phloretin and UDP-galactose as the activated sugar donor. Fullscan and MS/MS mass spectral
260 data were used to further characterize the products of the PGT2 reactions. Phloretin (Figure
261 4E) was detected as its pseudo-molecular ion m/z 273 [$M-1$]⁻, whereas trilobatin (Figure 4F),
262 3-OH phloretin (Figure 4G) and sieboldin (Figure 4H) were detected predominantly as the
263 corresponding formate adducts [M +formate]⁻¹. MS² on the formate adducts identified the
264 expected pseudo-molecular ion at m/z 435 and 451 [$M-1$]⁻ for the trilobatin and sieboldin
265 glucosides. MS³ on the m/z 435 and 451 [$M-1$]⁻ glucoside ions identified the m/z 273 and m/z
266 289 [$M-1$]⁻ ions of the phloretin and 3-OH phloretin aglycones, respectively.

267 PGT2 and PGT1 enzyme activities were compared over a pH range of 4–12 and with
268 temperatures from 15 to 60°C. The pH optimum of both enzymes was between pH 8.0–9.0
269 (Figure S5A, B), while the optimum temperature was ~40°C (Figure S5C, D). The K_m values
270 of PGT2 for phloretin were $18.0 \pm 6.7 \mu\text{M}$ ($V_{\text{max}} = 1.85 \pm 0.17 \text{ nmol}\cdot\text{min}^{-1}$) and for
271 UDP-glucose $103.6 \pm 23.0 \mu\text{M}$: ($V_{\text{max}} = 2.07 \pm 0.17 \text{ nmol}\cdot\text{min}^{-1}$) (Figure S5E, F). These K_m
272 values are comparable to those obtained for PGT1 for phloretin of $4.1 \pm 1.2 \mu\text{M}$ ($V_{\text{max}} = 1.54$
273 $\pm 0.08 \text{ nmol}\cdot\text{min}^{-1}$) and for UDP-glucose of $491 \pm 41 \mu\text{M}$ ($V_{\text{max}} = 8.84 \pm 0.35 \text{ nmol}\cdot\text{min}^{-1}$)
274 under the same purification conditions (Figure S5E, F).

275

276 **Expression of PGT2 and PGT3 in *Malus* spp.**

277 The relative expression of *PGT2* and *PGT3* were determined by RT-qPCR in the leaves of
278 nine *Malus* accessions (Figure 3). Three accessions produced predominantly trilobatin, three

279 both trilobatin and phloridzin, and three only phloridzin. *PGT2* was highly expressed in all six
280 *Malus* accessions producing trilobatin; however, expression was essentially absent in the three
281 accessions that did not synthesize trilobatin (Figure 3F). Conversely, the expression of *PGT1*
282 was high in the six *Malus* accessions producing phloridzin (Figure 3G). Expression of *PGT3*
283 was observed in all nine accessions, and did not correspond with the presence/absence of
284 trilobatin or phloridzin in the samples (Figure 3H).

285

286 **Structural Comparison of the Active Sites in PGT1-PGT3**

287 To investigate the structural basis for the difference in positional specificity for
288 glycosylation on phloretin, structural homology models were independently obtained for
289 PGT1-PGT3 using the iTASSER server (Yang and Zhang, 2015). The models were
290 superimposed and compared with the crystal structure of UGT72B1 bound with UDP-glucose
291 (donor) and 2,4,5-trichlorophenol (TCP, acceptor) (Brazier-Hicks et al., 2007) (PDB entry
292 2VCE). Overall, all structures were very similar, with RMSDs of ~ 1 Å between each other
293 (Figure S6). Sequence identities between PGT2/PGT1, PGT2/PGT3, and PGT1/PGT3 were
294 48, 86 and 47%, respectively. Around the predicted UDP binding site, however, the amino
295 acid conservation between the three enzymes was much higher (>95% identity) (Table S5),
296 consistent with the ability of these enzymes to bind the same donor molecule. Furthermore,
297 the positions of the catalytic dyad residues in the models (His16/Asp118 in PGT2 and PGT3,
298 His15/Asp118 in PGT1) were in excellent agreement with the crystal structure of UGT72B1.
299 In contrast, conservation between PGT2 and PGT1 was considerably lower among the amino
300 acids shaping the acceptor binding pocket (23% identity; 3/13 residues) (Figure 5A, B).
301 Similarly, although less pronounced, conservation between PGT2 and PGT3 around the
302 acceptor binding pocket dropped to 69% (9/13 residues) (Figure 5B, C).

303

304 **Metabolic Engineering of Trilobatin Production in *N. benthamiana***

305 To reconstitute the full apple pathway for trilobatin and phloridzin production in *Nicotiana*
306 *benthamiana*, *MdMyb10* and two biosynthetic genes *MdDBR* and *MdCHS* were transiently
307 expressed together to catalyze the synthesis of phloretin substrate for glycosylation. Leaves
308 infiltrated with *MdMyb10*, *MdDBR*, *MdCHS* and *PGT2* were analyzed by Dionex-HPLC and

309 exhibited a peak at 32 min that corresponded to the trilobatin standard (Figure 6A, B), whilst
310 those infiltrated with *PGT1* exhibited a peak at 27.2 min corresponding to phloridzin (Figure
311 6C, D). Concentrations of trilobatin produced with *PGT2* and phloridzin produced with *PGT1*
312 were similar (45 vs 87 $\mu\text{g}\cdot\text{g}^{-1}$ respectively; Table S6). Neither phloridzin nor trilobatin was
313 detected in leaves inoculated with the GUS control vector (Figure 6E). Interestingly, no
314 phloretin was detected in the reactions, suggesting that glycosylation is needed to stabilize the
315 reactive phloretin in *N. benthamiana* leaves.

316 *MdDBR* and *MdCHS1* were required for synthesis of trilobatin in co-infiltrations with
317 *PGT2* (Table S6). Substitution of *MdDBR* for *MdENRL3* (Dare et al., 2013a) abolished
318 trilobatin production. The *MdMyb10* transcription factor increased trilobatin formation
319 presumably via increased substrate flux through the phenylpropanoid pathway (Table S6).
320 These results indicate that three *Malus* biosynthetic genes and a transcription factor are
321 sufficient to reconstitute the pathway to trilobatin and phloridzin production in *N.*
322 *benthamiana* (and likely any other plant) for biotechnological applications.

323

324 **Over-expression of *PGT2* in *M. × domestica***

325 *PGT2* was over-expressed in *M. × domestica* backgrounds GL3 and ‘Royal Gala’. Fourteen
326 transgenic GL3 lines were obtained and *PGT2* expression was significantly increased in the
327 leaves of 4-week-old plants from eight lines (# 1, 4, 5, 6, 7, 9, 11, 14) compared with wildtype
328 (Figure 7A). Amounts of trilobatin were significantly increased in the same eight lines + line
329 #10 compared with wildtype, with concentrations ranging from ~5 to 11 $\text{mg}\cdot\text{g}^{-1}$ FW (Figure
330 7B). No significant differences were observed in phloridzin, phloretin (Figure 7B) or total
331 content of trilobatin + phloridzin (Figure S7A) among the GL3 transgenic lines. Eleven
332 transgenic ‘Royal Gala’ lines over-expressing *PGT2* were also regenerated. An initial screen
333 of shoots in tissue culture showed that all transgenic lines contained increased concentrations
334 of trilobatin (Figure S8A), but similar total DHC content (Figure S8B) compared with
335 wildtypes. Further analysis of the young leaves from six of the ‘Royal Gala’ lines grown in a
336 containment glasshouse confirmed these results (Figure S8C and Figure S8D).

337 The relative expression of *PGT1*, *MdCHS* and *PGT3* were also analyzed by RT-qPCR in
338 the GL3 transgenic *PGT2* over-expression lines. The expression levels of *PGT1* (Figure S7B)

339 and *MdCHS* (Figure S7C) were not significantly altered in the 14 transgenic apple lines.
340 Interestingly, the relative expression of *PGT3* in all 13/14 transgenic GL3 lines decreased
341 significantly (Figure S7D). Strongest suppression was observed in lines expressing *PGT2* and
342 trilobatin at the lowest levels, suggesting co-suppression of the endogenous *PGT3* gene by the
343 introduced *PGT2* transgene.

344

345 **Physiology of *PGT2* Over-expression Lines Grown under Simulated Field Conditions**

346 Manipulation of dihydrochalcone levels in some transgenic apple lines has been shown to
347 severely affect plant morphology (Dare et al., 2013b; Dare et al., 2017; Zhou et al., 2019).
348 Multiple seedlings of three *PGT2* over-expression lines (#'s 1, #5 and #14) and matching
349 wildtypes were assessed for changes in morphology at eighteen months of age when grown
350 under simulated field conditions. No significant differences were observed in plant height
351 (Figure 8A, B), total number of branches per tree (Figure 8C), leaf morphology (Figure 8D)
352 or fresh weight per leaf (Figure 8E).

353 Changes in dihydrochalcone levels have also been implicated in pathogen susceptibility in
354 some transgenic apple lines (Hutabarat et al., 2016; Zhou et al., 2019), but not in others
355 (Gosch et al., 2012). *PGT2* over-expression lines and matching wildtypes grown under
356 simulated field conditions were subject to natural pathogen infection; no disease or pest
357 management schemes were imposed on the plants. Under these conditions, no differences in
358 disease susceptibility were observed between the *PGT2* transgenics and wildtypes. The most
359 common infection on all plants was by powdery mildew (Figure 8F), but no significant
360 differences in powdery mildew infection rate were observed (Figure 8G).

361

362 **Sensory Evaluation of Apple Leaf Teas from *PGT2* Transgenic Plants**

363 Sensory analysis was used to investigate the impact of *PGT2* over-expression on the taste
364 of apple leaf tea. Leaves were harvested from 4-month-old wildtype GL3 plants and two
365 transgenic lines (#'s 1, 9). After drying, the phloridzin contents in the wildtype and transgenic
366 leaves were similar ($\sim 150 \text{ mg}\cdot\text{g}^{-1}$ DW). The transgenic lines also contained trilobatin (~ 100
367 $\text{mg}\cdot\text{g}^{-1}$ DW), whilst wildtype contained none (Figure 9A). After steeping, $\sim 27\%$ of the
368 phloridzin and 16% of the trilobatin was extracted into the tea (Figure 9A).

369 In triangle tests, panelists were clearly able to distinguish the flavor of tea produced from
370 the transgenic *PGT2* leaves compared with tea produced from wildtype ($p < 0.01$, 38 correct
371 observations out of $n = 70$). To determine the basis for this discrimination, panelists were then
372 asked to rate the sweetness of each sample on a scale from 1–10. The average sweetness of
373 the two transgenic lines was rated significantly ($p < 0.05$, $n = 23$) higher at 4.8 and 4.6
374 respectively, compared with that of wildtype, rated at 3.2.

375

376 **DISCUSSION**

377 Glycosyltransferases are encoded by large gene families, and identifying enzymes with
378 specific activities based on homology is difficult. Two enzymes capable of 4'-*O*-glycosylation
379 of phloretin in vitro have been reported (Gosch et al., 2012; Yahyaa et al., 2016), but these
380 genes are expressed in tissues that produce only phloridzin. In this study, we used multiple
381 approaches to show that *PGT2* is responsible for production of trilobatin in apple. The genetic
382 locus for trilobatin production co-located with the *PGT2* gene, and HRM markers developed
383 to *PGT2* segregated strictly with trilobatin production. Molecular and biochemical analysis
384 demonstrated that *PGT2* was only expressed in accessions where trilobatin (or sieboldin) was
385 produced and that the enzyme showed Ph4'-oGT activity in vitro. Finally, over-expression of
386 *PGT2* in domesticated apple confirmed that *PGT2* leads to the production of trilobatin in
387 planta.

388 The modeling results for PGT1-PGT3 showed strong amino acid conservation between the
389 three enzymes around the predicted UDP binding site, a feature common to the UGT
390 superfamily (Li et al., 2001). Although both are members of the UGT88 family, PGT2
391 (UGT88A32) and PGT1 (UGT88F1) showed large variations in the amino acid composition
392 of their respective acceptor binding pockets, which is consistent with these two enzymes
393 having different activities and generating different products. More surprisingly, PGT2 and
394 PGT3 (UGT88A32), which are putative paralogs and share high amino acid identity, also
395 show strong differences in overall activity and specificity. In the case of PGT3, the 3D model
396 analysis suggests that the low enzymatic activity may be due to one (or to a combination) of
397 the four amino acids differing with PGT2 in the acceptor binding pocket. Among these, the
398 substitution at position 145 of an Asn in PGT2 for a bulkier Phe in PGT3 may restrict the size
399 of the pocket and impair the binding of the acceptor. However, site-directed mutagenesis
400 and/or crystallographic work is required to confirm this hypothesis and to further understand
401 the Ph2'-oGT activity of PGT3, compared with the Ph4'-oGT activity of PGT2.

402 UGTs with the ability to glycosylate phloretin have been described in *M. domestica* from
403 multiple UGT families (Jugd e et al., 2008; Gosch et al., 2010; Yahyaa et al., 2016; Zhou et al.,
404 2017; Elejalde-Palmett et al., 2018). However, the majority, including the *PGT2* and *PGT3*,
405 belong to the UGT88 family (for a phylogeny see Figure S9). The absence of trilobatin

406 biosynthesis in *M. × domestica* is not due to mutations in the *PGT2* gene, as a complete ORF
407 was amplified from ‘Fuji’ and shown to be identical to the *PGT2* ORF from *M. toringoides* (a
408 species producing trilobatin). Instead, DGE and RT-qPCR analyses indicated that the mutation
409 was at the transcriptional level, with *M. × domestica* expressing *PGT2* at very low levels. *M.*
410 *× domestica* and all other accessions tested do express the putative *PGT3* paralog located
411 within ~10 kb of *PGT2*. However, despite high homology, *PGT3* does not exhibit Ph4'-oGT
412 activity, but weak Ph2'-oGT activity. The *Pyrus* (pear) genome (Linsmith et al., 2019)
413 contains a close homolog of the *PGT3* gene (XP_009368718.2), but not *PGT2*, suggesting
414 that the *PGT2* gene may have evolved recently only in the *Malus* lineage, or have been lost
415 from the *Pyrus* lineage. The absence of trilobatin production in *M. × domestica* does not
416 appear to be driven by domestication, as a number of wild apple species (e.g. *M. baccata*;
417 Figure 3F) produce only phloridzin and lack expression of *PGT2*. Most wild *Malus* species
418 that express *PGT2* accumulate sieboldin, or trilobatin in combination with phloridzin. Only
419 one species expressing *PGT2*, *M. trilobata*, accumulates trilobatin alone.

420 Manipulation of dihydrochalcone levels in transgenic apples has been associated with
421 changes in plant physiology, notably in plant morphology (Dare et al., 2017), and
422 susceptibility to pathogen infection (Gosch et al., 2012; Hutabarat et al., 2016; Zhou et al.,
423 2019). Transgenic *PGT2* over-expressing lines appeared phenotypically normal, and no
424 differences in disease susceptibility were observed between the *PGT2* transgenics and
425 wildtypes grown under simulated field conditions. In transgenic apple seedlings
426 over-expressing chalcone 3'-hydroxylase, total DHC content was not altered, but reduced
427 susceptibility to both fire blight and apple scab was associated with an increase (up to 11.5%)
428 in 3-hydroxyphloridzin accumulation (Hutabarat et al., 2016). In the *PGT2* transgenics, total
429 DHC content was similarly not altered, but trilobatin accumulation (up to 38%) did not alter
430 disease susceptibility. This difference may suggest that sieboldin is more effective in
431 promoting disease resistance. However, in Hutabarat et al., (2016) pathogen sensitivity assays
432 were performed using artificial shoot inoculations and it was not reported if increased
433 sieboldin concentrations altered susceptibility under field conditions. Conversely, our
434 observations do not preclude the possibility that disease susceptibility in the *PGT2* transgenics

435 will change as the plants age, or that the plants were not exposed to pathogens sensitive to
436 trilobatin under simulated field conditions.

437 Sensory analysis of apple leaf teas made from transgenic plants over-expressing *PGT2*
438 demonstrated that they could be clearly distinguished from teas made from wildtype apple
439 leaves. The concentrations of trilobatin extracted into tea (Figure 9A, $\sim 150 \text{ mg}\cdot\text{L}^{-1}$) were
440 above the sweetness detection threshold reported for trilobatin ($3\text{--}200 \text{ mg}\cdot\text{L}^{-1}$) (Jia et al.,
441 2008). The perception of increased sweetness in the transgenic leaf teas was consistent with
442 increased production of trilobatin and not a decrease in concentrations of bitter-tasting
443 phloridzin. However, a more detailed analysis by trained panelists would be required to
444 understand the sensory properties fully. An iso-sweetness comparison test between trilobatin
445 purified from leaves of the crabapple hybrid ‘Adams’ and sucrose indicated that trilobatin was
446 ~ 35 -fold sweeter than sucrose (Figure 9B). This number is slightly lower than figures reported
447 previously (Jia et al., 2008), which may relate to the purity of the trilobatin tested, the delivery
448 system, or variation in panelist sensitivity to sucrose or trilobatin.

449 Identification of the Ph4'-oGT for trilobatin production will allow us to investigate
450 whether *PGT2* over-expression in the fruit affects consumer perception of sweetness.
451 Transgenic ‘Royal Gala’ plants over-expressing the *PGT2* gene have been produced and these
452 contain both trilobatin and phloridzin in the leaves. This result indicates that *PGT2* is
453 reasonably competitive with *PGT1* for the pool of phloretin substrate available in leaves and
454 that *PGT2* should be competitive with *PGT1* for the smaller pool of phloretin produced in
455 fruit. This hypothesis will be tested when the transgenic ‘Royal Gala’ plants reach maturity in
456 several years’ time. An alternative approach to increasing trilobatin production in *M. ×*
457 *domestica* would be to use molecular markers to accelerate the introgression of *PGT2* into
458 elite breeding material. However, for this approach to be successful, parental material in
459 which *PGT2* is well-expressed in fruit (rather than leaves and flowers) needs to be identified.

460 Identification of the Ph4'-oGT for trilobatin production and reconstitution of the apple
461 pathway to trilobatin and phloridzin production in *N. benthamiana* may also allow high
462 amounts of trilobatin to be produced via biotechnological means, such as biopharming and
463 metabolic engineering in yeast. The utility of this approach has already been demonstrated for
464 *PGT1* in yeast (Eichenberger et al., 2016), but not in planta. The ability to produce large

465 quantities of trilobatin would allow it to be tested not only as a natural sweetener in the food
466 and beverage industry, but also for its potential health benefits (Fan et al., 2015; Xiao et al.,
467 2017).

468

469 **MATERIALS AND METHODS**470 **Plant Material**

471 Trilobatin production was mapped in an F1 seedling population between ‘Royal Gala’ and
472 Y3 grown in a greenhouse at PFR, Auckland, New Zealand. Y3 is derived from the crabapple
473 hybrid ‘Aotea’ x *M. × domestica* ‘M9’. ‘Aotea’ is an open-pollinated *M. sieboldii* (which
474 produces sieboldin) selection. *M. trilobata* and ‘Aotea’ were grown at the PFR research
475 orchard in Havelock North, New Zealand.

476 *M. micromalus* ‘Makino’ and the F1 population for differential gene expression analysis
477 between the crabapple hybrid ‘Radiant’ and *M. × domestica* ‘Fuji’ were grown at the
478 Luochuan Apple Experimental Station, Northwest A&F University, Shaanxi, China. All other
479 material was grown in an experimental orchard at Northwest A&F University, Yangling,
480 Shaanxi, China. All trees were grown on their own roots and managed using standard
481 horticultural growth practices and management for disease and pest control.

482 For physiological experiments on transgenic lines, GL3 and wildtype plants were grown in
483 a plastic tunnel house in a randomized layout at Northwest A&F University. To meet
484 transgenic containment restrictions, plants were grown in pots (height 22 cm, diameter 32 cm).
485 To simulate field conditions, plants were grown under ambient temperature and
486 environmental conditions. As the tunnel house was open ended, plants were subject to natural
487 pathogen infection. No disease or pest management schemes were imposed.

488

489 **Chemicals**

490 Trilobatin was purified from the crabapple hybrid ‘Adams’ (Xiao et al., 2017). Sieboldin,
491 3-OH phloretin and quercetin glycosides were purchased from PlantMetaChem (www.
492 PlantMetaChem.com) and cyanidin from Extrasynthese (www.extrasynthese.com). All other
493 chemicals, including phloridzin and phloretin, were obtained from Sigma Aldrich
494 (sigmaaldrich.com).

495

496 **Mapping the *Trilobatin* Locus**

497 Leaf tissue from seedlings in the ‘Royal Gala’ x Y3 population were harvested and
498 weighed before snap-freezing in liquid nitrogen. Phenolics were extracted from 100–250 mg

499 of leaf tissue as described by Dare et al., (2017) and polyphenols quantified by Dionex-HPLC
500 on an Ultimate 3000 system (Dionex, Sunnyvale, CA, USA) equipped with a diode array
501 detector at 280 nm as described by André et al., (2012). Seedling DNA was extracted using
502 the DNaseasy Plant Mini Kit (Qiagen) and genotypes determined using the IRSC 8K SNP
503 array (Chagné et al., 2012). The SNP array data were analyzed using the Genotyping Module
504 of the GenomeStudio Data Analysis Software (Illumina). The genetic map was constructed
505 using JoinMap version 4.0 and the position of the *Trilobatin* locus on LG7 of Y3 was
506 identified after conversion of SNP physical coordinates in the ‘Golden Delicious’ v1.0
507 genome assembly (upon which the IRSC 8K SNP array was designed) to the latest version of
508 the apple reference genome (GDDH13 v1.1). The position of *PGT2* was then defined using
509 HRM primers designed within the *PGT2* candidate genes (Figure 1, Table S3) and PCR
510 conditions as in Chagné et al., (2008).

511

512 **Activity-directed Protein Purification**

513 A detailed protocol for activity-directed purification of Ph4'-oGT activity from apple
514 flower petals is given in the legend to Table S1. Purified protein fractions were separated on
515 12% (w/v) SDS-PAGE gels and visualized by Coomassie Blue R-250 staining. Target bands
516 were cut and digested in gel with trypsin according to the method of Gao et al., (2017). The
517 peptide mixture was then loaded onto a reverse phase trap column (Thermo Scientific
518 Acclaim PepMap 100, 100 μm x 2 cm, nanoViper C18) connected to the C18-reversed phase
519 analytical column (Thermo Scientific Easy Column, 10 cm long, 75 μm inner diameter, 3 μm
520 resin) in buffer A (0.1% (v/v) formic acid) and separated with a linear gradient of buffer B
521 (84% (v/v) acetonitrile and 0.1% (v/v) formic acid) at a flow rate of 300 $\text{nL}\cdot\text{min}^{-1}$ controlled
522 by IntelliFlow technology. LC-MS/MS analysis was performed on a Q Exactive mass
523 spectrometer (Thermo Scientific) that was coupled to Easy nLC (Proxeon Biosystems, now
524 Thermo Scientific) for 60 min, and the mass spectrometer was operated in positive ion mode.
525 Details of MS/MS spectra analysis are given in the legend to Table S1.

526

527 **Differential Gene Expression Analysis**

528 The F1 population developed from a cross between the crabapple hybrid ‘Radiant’ and *M.*

529 × *domestica* ‘Fuji’ was screened for trilobatin and phloridzin by HPLC. Eighty-one plants
530 containing trilobatin + phloridzin (T+P) and 81 plants containing only phloridzin (P) were
531 identified. One expanding leaf was collected from each seedling (~20 cm tall) and three
532 pooled replicate samples for T+P and P were prepared (each replicate containing leaves from
533 27 plants). Total RNA was extracted from frozen ground powder using Trizol Reagent (Life
534 Technologies) following the manufacturer’s instructions and checked for RNA integrity on an
535 Agilent Bioanalyzer 2100. Sequencing libraries were generated from 3 µg RNA per sample
536 using NEBNext Ultra RNA Library Prep Kit for Illumina (Thermo Fisher) following the
537 manufacturer’s recommendations and index codes were added to attribute sequences to each
538 sample. RNA was sequenced by Novogene (Beijing, China) using the Illumina HiSeq4000
539 platform. Details of sequence alignment and differential gene expression analysis are given in
540 the legend to Table S2.

541

542 **RT-qPCR Analysis**

543 Total RNA was extracted from young leaves as described by Malnoy et al., (2001).
544 First-strand cDNA was synthesized from 1 µg of total RNA using the PrimeScript RT Reagent
545 Kit (Takara, Dalian, China), according to the manufacturer’s instructions. RT-qPCR was
546 performed with a Bio-Rad CFX96 system (Bio-Rad Laboratories, Hercules, CA, USA) using
547 the TB Green Premix Ex Taq (Takara, Dalian, China). *MdACTIN* was used as the reference
548 gene. The relative expression levels were calculated according to the $2^{-\Delta\Delta CT}$ method (Livak
549 and Schmittgen, 2001). Three biological replicates each with three technical repeats were used
550 for RT-qPCR analysis. Gene-specific primers are listed in Table S3.

551

552 **Biochemical Characterization of *PGT1-3* in *E. coli***

553 The ORFs of *PGT1-3* were amplified using primers in Table S3 and ligated into pET28a(+)
554 using the One Step Cloning Kit (www.vazyme.com). Recombinant proteins were expressed in
555 *E. coli* BL21 (DE3) cells with 0.5 mM isopropyl-1-thio-β-galactopyranoside (IPTG) at 16°C
556 for 24 h at 80 rpm. Purification of recombinant proteins was performed using Ni-NTA agarose
557 (Millipore). Eluted fractions were used for determining enzyme activity and for SDS-PAGE
558 analysis (Figure S10). Active fractions were concentrated using Vivaspin 2 concentrators

559 (Sartorius, Germany).

560 GT activity assays were performed in triplicate in 200 μ L reactions containing 50 mM
561 Tris-HCl (pH 9.0), 1 mM DTT, 0.5 mM phloretin, 0.5 mM UDP-glucose, and 30–80 ng
562 enzyme. Reaction mixtures were incubated for 10 min at 40°C and reactions stopped by
563 adding 40 μ L of 1 M HCl. NaOH (1 M) was used to adjust the pH to neutral for HPLC
564 analysis of the products at 280 nm.

565

566 HPLC and LC-MS/MS Analysis of Phenolic Compounds

567 Leaf tissue (500 mg) for HPLC was snap frozen in liquid nitrogen, and extracted with 1.5
568 mL of a solution containing 50% (v/v) methanol and 2% (v/v) formic acid at 0–4°C. The
569 homogenate was centrifuged at 10,000 g for 10 min, and the supernatant used for HPLC after
570 filtering with a 0.45 μ M syringe (Li et al., 2013). Polyphenols were quantified on a LC-20A
571 liquid chromatograph equipped with a diode array detector (Shimadzu Corporation, Tokyo,
572 Japan) at 280 nm as described previously (Zhang et al., 2018).

573 For LC-MS/MS analysis, scaled up reactions were performed containing approximately 10
574 μ g enzyme, 10 μ M substrate and UDP-glucose at a final concentration of 250 μ M. Reactions
575 were performed in triplicate, and stopped after 1 h by addition of 10 μ L of 10% (v/v) glacial
576 acetic acid and blown down to dryness under a gentle stream of N₂. The reaction products
577 were reconstituted in 100 μ L 5:95 (v/v) acetonitrile: water + 0.1% (v/v) formic acid, and then a
578 10 μ L aliquot taken which was diluted 10-fold in the same solvent. LC-MS/MS employed an
579 LTQ linear ion trap mass spectrometer fitted with an ESI interface (Thermo Scientific)
580 coupled to an Ultimate 3000 UHPLC and PDA detector (Dionex).

581 Phenolic compound separation was achieved using a Hypersil Gold aQ 1.9 μ (Thermo
582 Scientific), 150 \times 2.1 mm analytical column maintained at 45°C. Solvents were (A) water +
583 0.1% (v/v) formic acid and (B) acetonitrile + 0.1% (v/v) formic acid and the flow rate was 200
584 μ L \cdot min⁻¹. The initial mobile phase, 5% B/95% A, was held for 2 min then ramped linearly to
585 15% B at 10 min, held for 3.75 min, before ramping linearly to 25% B at 18 min, 33% B at 25
586 min, 50% B at 28 min, 100 % B between 29 and 32 min before resetting to the original
587 conditions. The sample injection volume was 2 μ L. MS data were acquired in the negative
588 mode using a data-dependent LC/MS³ method. This method isolates and fragments the most

589 intense parent ion to give MS² data, then isolates and fragments the most intense daughter ion
590 (MS³ data). The ESI voltage, capillary temperature, sheath gas pressure and sweep gas were set
591 at -10 V, 275°C, 35 psi and 5 psi, respectively.

592

593 **Molecular Modeling**

594 The sequences for PGT1–3 were independently submitted to the iTASSER server (Yang
595 and Zhang, 2015). C-scores of the best models used for structural analysis were -0.38, 0.94
596 and 1.52 for PGT1, 2 and 3, respectively. Superimposition, structural analysis and figures
597 were performed using the PyMOL Molecular Graphics System, Version 2.0 (Schrödinger,
598 LLC).

599

600 **Transient Expression in *N. benthamiana***

601 *PGT2* was amplified from *M. trilobata*, pHEX2-*MdCHS* and *MdDBR* (Yahyaa et al., 2016)
602 from ‘Royal Gala’ using the primers in Table S3. Genes were cloned into pHEX2 to generate
603 the binary vectors pHEX2-*PGT2*, pHEX2-*CHS* and pHEX2-*DBR* respectively. Construction
604 of pHEX2-Myb10, pGreen0029-ENRL3, pBIN61-p19 (containing the suppressor of gene
605 silencing p19) and the control construct pHEX2-GUS have been reported previously (Espley
606 et al., 2007; Dare et al., 2013a; Nieuwenhuizen et al., 2013). All constructs were
607 electroporated in *Agrobacterium tumefaciens* strain GV3101. Freshly grown cultures were
608 mixed in equal ratio and infiltrated into *Nicotiana benthamiana* leaves as described in Hellens
609 et al., (2005). After 7 d, leaves were harvested and phenolic compounds extracted for
610 Dionex-HPLC analysis.

611

612 **Generation of Transgenic Apple Plants**

613 The coding region of *PGT2* was amplified from *M. toringoides* using the primers in Table
614 S3 and cloned into pCAMBIA2300 using the One Step Cloning Kit (www.vazyme.com). The
615 *PGT2*:pCAMBIA plasmid was then transformed into *Agrobacterium tumefaciens* (strain
616 GV3101) cells. Transgenic GL3 apple plants were generated by *Agrobacterium*-mediated
617 transformation according to Dai et al.; (2013) and Sun et al.; (2018). Transgenic ‘Royal Gala’
618 plants were transformed with pHEX2-*PGT2* and plants regenerated as described previously

619 (Yao et al., 1995; Yao et al., 2013).

620

621 **Sensory Panel Analysis**

622 Apple leaves from wildtype and two *PGT2* transgenic GL3 lines were washed with water
623 and dried at room temperature. Leaves were held at 200°C for 1 min to inactivate enzymes,
624 then dried at 80°C in an oven for 60 min. Apple leaf tea was made using 5 g of dried leaves
625 with the ratio of leaves:water being 1:100 (g:mL). Water at ~80°C was added to the leaves for
626 15 min, then all leaves were removed to stop further extraction. The tea was then kept at 50°C
627 in water bath for sensory analysis. The sensory panel consisted of 23 individuals and included
628 14 females and 9 males (all 20–30 years of age). Participation was voluntary and all
629 participants gave their written consent prior to participation in the study. For the triangle tests,
630 participants were given three trays, each tray had three cups (2 mL tea in each cup) with
631 transgenic and wildtype leaf tea in a random design, either two transgenic and one wildtype or
632 two wildtype and one transgenic. Participants were asked to sequentially taste the three
633 samples on each tray and select which sample was different. To assess the relative sweetness
634 of wildtype vs transgenic apple leaf teas, two samples (one transgenic and one wildtype) were
635 presented and the 23 panelists were asked to score the two samples on a sweetness scale from
636 1 to 10. For all the tasting tests, participants kept the samples in their mouths for 1–2 seconds,
637 then spat them out into a waste container. Participants rinsed their mouths between samples
638 with water and a dry biscuit was provided between each sample set.

639 Five participants with high acuity for trilobatin in the triangle test were selected to perform
640 the iso-sweetness comparison test between trilobatin and sucrose. Each participant was given
641 one trilobatin solution and eight sucrose solutions at different concentrations to taste.
642 Solutions were prepared as described above for the apple leaf teas. The trilobatin solutions
643 were presented at 12.3, 18.5, 27.8 and 41.7 mg per 100 mL, while the sucrose solutions were
644 presented at 296.3, 444.4, 592.6, 666.7, 888.9, 1000, 1333.3 and 2000 mg per 100 mL.

645 **ACCESSION NUMBERS**

646 Nucleotide sequences for genes characterized as part of this study were deposited in
647 GenBank and received the accession numbers MN38099-MN381012.

648

649 **SUPPLEMENTAL DATA**

650 The following supplemental materials are available.

651 **Supplemental Figure S1:** HRM profiles of the four SNP markers located at the *Trilobatin*
652 locus.

653 **Supplemental Figure S2.** Amino acid alignment of *PGT2* sequences from *Malus* accessions.

654 **Supplemental Figure S3.** Amino acid alignment of *PGT3* sequences from *Malus* accessions.

655 **Supplemental Figure S4:** LC-MS/MS analysis of reactions containing *PGT2*, quercetin and
656 UDP-glucose.

657 **Supplemental Figure S5:** Biochemical properties of recombinant *PGT2* and *PGT1*.

658 **Supplemental Figure S6:** 3D-superimposition of PGT1, 2 and 3 models with the UGT71B1
659 crystal structure.

660 **Supplemental Figure S7:** HPLC and RT-qPCR analysis of transgenic GL3 plants
661 over-expressing *PGT2*.

662 **Supplemental Figure S8:** HPLC analysis of transgenic ‘Royal Gala’ plants over-expressing
663 *PGT2*.

664 **Supplemental Figure S9:** Phylogeny of UDP-glycosyltransferases.

665 **Supplemental Figure S10:** SDS-PAGE of recombinant PGT2 and PGT1 proteins..

666 **Supplemental Table S1:** Proteins identified after activity-directed purification of Ph4'-oGT
667 activity.

668 **Supplemental Table S2:** Differential gene expression analysis in tissues high in trilobatin but
669 low in phloridzin.

670 **Supplemental Table S3:** Primer sequences for HRM analysis, RT-qPCR and cloning.

671 **Supplemental Table S4:** Phenotype-to-genotype comparisons for individuals used to
672 construct the genetic map and in HRM assays.

673 **Supplemental Table S5:** Amino acids surrounding the donor and acceptor binding sites in
674 PGT1–3, identified from the respective 3D models.

675 **Supplemental Table S6:** Transient production of dihydrochalcones in *N. benthamiana*.

676

677 **ACKNOWLEDGEMENTS**

678 We thank Monica Dragulescu and her team for plant care at PFR, Shanshan Zhao, Xiaohui
679 Cui and Ruijia Yang for help running the sensory trial and Andrew Dare, Cecilia Deng and
680 Sue Gardiner for reviewing the manuscript.

681

682 **Table 1: Proteins Identified after Activity-directed Purification**

Protein	Description	iBAQ R1	iBAQ R2
MDP0000836043/ MDP0000318032	<i>M. × domestica</i> UDP-glycosyltransferase 88A1-like	3786800000	3146000000
MDP0000155691	<i>M. × domestica</i> pentatricopeptide repeat-containing protein At4g14190, chloroplastic	96169000	33639000
MDP0000267350	<i>M. × domestica</i> monodehydroascorbate reductase-like	85148000	273050000
MDP0000705244	<i>M. × domestica</i> UDP-glycosyltransferase 76B1-like	75047000	628300
MDP0000234480	<i>M. × domestica</i> transaldolase-like	31272000	246460000

683

684 Abundant proteins identified by LC-MS/MS analysis of bands isolated after activity-directed
685 purification of Ph4'-oGT activity from flowers of the crabapple hybrid 'Adams' (containing
686 trilobatin and not phloridzin). IBAQ = sum of all peptide intensities divided by the number of
687 observable peptides of a protein. The analysis was performed twice and the most abundant
688 proteins found in both analyses are given as R1 and R2.

689

690 **Table 2: Differentially Expressed Genes.**

Gene	Description	log2-fold change
MDP0000836043	<i>M. × domestica</i> UDP-glycosyltransferase 88A1-like (LOC103410306), mRNA	7.54
MDP0000204525	<i>M. × domestica</i> cinnamoyl-CoA reductase 1 (LOC103427062), mRNA	6.89
MDP0000206483	<i>M. × domestica</i> cytokinin hydroxylase-like (LOC114826167), mRNA	6.77
MDP0000219066	<i>M. × domestica</i> cytochrome P450 CYP72A219-like (LOC103427349), mRNA	6.68
MDP0000737403	<i>M. × domestica</i> probable mannitol dehydrogenase (LOC103446373), mRNA	6.63

691

692 The five most differentially expressed genes identified after transcriptome analysis of pooled
 693 leaf samples of an F1 population between the crabapple hybrid ‘Radiant’ (containing both
 694 trilobatin and phloridzin) and *M. × domestica* ‘Fuji’ (containing only phloridzin).

695

696 **Table 3. Substrate Specificity of Recombinant PGT2 Cloned from *M. toringoides*.**

Substrate	Product	Conversion (%)
phloretin	trilobatin	100.0±6.1
3-OH phloretin	sieboldin	58.7±2.3
quercetin	quercetin 3- <i>O</i> -glucoside	9.1±0.1
phloridzin	Nd	0
trilobatin	Nd	0
sieboldin	Nd	0
naringenin	Nd	0
cyanidin	Nd	0
caffeic acid	Nd	0
4-coumaric acid	Nd	0
neohesperidin	Nd	0
chlorogenic acid	Nd	0
boiled protein	Nd	0

697

698 The products of reactions using UDP-glucoside as the sugar donor and the twelve substrates
699 shown were determined by LC-MS/MS. Conversion % is the amount of product formed
700 relative to the conversion of phloretin to trilobatin which was set at 100%. nd = no products
701 detected. All reactions were performed in triplicate.

702

703 **FIGURE LEGENDS**704 **Figure 1. Activity-directed Purification of Ph4'-oGT Activity from Flowers of the**
705 **Crabapple Hybrid 'Adams'.**

706 Active fractions are shown as dark gray bars. (A) Purification by Q-sepharose
707 chromatography. (B) Purification by phenyl sepharose chromatography using pooled fractions
708 from Q-sepharose. (C) Purification by Superdex 75 chromatography using pooled fractions
709 from phenyl sepharose. Protein concentration (280 nm), enzyme activity, pooled fractions and
710 NaCl or (NH₄)₂SO₄ gradient in the elution buffer are indicated. (D) SDS-PAGE analysis of the
711 four active fractions after purification by Superdex 75 chromatography are shown in lanes 1–4.
712 M = Premixed Broad protein marker (Takara, Dalian, China). Arrow indicates the band sent
713 for LC-MS/MS analysis.

714

715 **Figure 2. Genetic Mapping of Trilobatin production in a 'Royal Gala' x Y3 Segregating**
716 **Population.**

717 (A) The *Trilobatin* locus was mapped near the base of LG7 of Y3 using the IRSC 8K SNP
718 array (Chagné et al., 2012). Genetic locations in centiMorgan (cM) are shown on the left and
719 physical location in base pairs on the right (based on the 'Golden Delicious' doubled-haploid
720 assembly GDDH13 v1.1). The physical locations of three HRM-SNP markers (Figure S1;
721 Table S3) are indicated. (B) The genomic region of the *Trilobatin* locus in the 'Golden
722 Delicious' v1.0p assembly (top) and the doubled-haploid assembly GDDH13 v1.1 (bottom).
723 The physical positions of two UDP-glucosyltransferase genes identified at the locus in each
724 assembly are shown below the gene model. The black arrow corresponds to *PGT2*, the
725 speckled arrow to *PGT3* and the gray arrow to MD07G1280900 (annotated as a suppressor of
726 auxin resistance). N.B. *PGT2* in the doubled-haploid assembly was incorrectly annotated as
727 two truncated gene models MD07G1281000 and MD07G1281100. N.B. HRM1 and 3
728 amplified on both genes.

729

730 **Figure 3. Biochemical and Expression Analysis of *PGT1–3*.**

731 (A) Authentic standards of P = phloridzin, T = trilobatin and Pt = phloretin compared with the
732 products formed by recombinant *PGT2* from *M. toringoides* (B), *PGT3* from *M. sieboldii* (C),

733 PGT1 from *M. × domestica* ‘Fuji’ (D) and an empty vector control (E) in the presence
734 phloretin and UDP-glucose. Experiments were performed in triplicate and a single
735 representative trace is shown. Expression of *PGT2* (F), *PGT3* (G) and *PGT1* (H) were
736 analyzed by RT-qPCR using gene-specific primers (Table S3) in three *Malus* accessions
737 containing only trilobatin (black bars), three containing trilobatin and phloridzin (white bars),
738 and three containing only phloridzin (gray bars). *MdACTIN* was used as the reference gene.
739 RG = ‘Royal Gala’. Data are means (\pm SE) of three biological replicates from young leaves.
740 Expression is presented relative to *M. × domestica* ‘Fuji’ in (F) and (G) and to *M. toringoides*
741 in (H) (values set as 1).

742

743 **Figure 4. LC-MS/MS Analysis of Products Formed by *PGT2*.**

744 Base peak plots: (A) mixed standard of phloretin (Pt) and trilobatin (T); (B) *PGT2* + phloretin
745 + UDP-glucose; (C) mixed standard of 3-OH phloretin (3Pt) + sieboldin (S); (D) *PGT2* +
746 3-OH phloretin + UDP-glucose; Mass spectra for reaction products and standards: (E)
747 fullscan, MS² and MS³ data for phloretin; (F) fullscan, MS² and MS³ data for trilobatin; (G)
748 fullscan, MS² and MS³ data for 3-OH phloretin; and H) fullscan, MS² and MS³ data for
749 sieboldin.

750

751 **Figure 5. Structural Comparison of the Acceptor Binding Pockets of PGT1–PGT3** 752 **Models.**

753 The models were constructed by the iTASSER server. PGT1 (A) and PGT3 (C) residues
754 labelled in red are different from PGT2 (B). The TCP (2,4,5-trichlorophenol) acceptor (shown
755 in gray) from the UGT72B1 co-crystal structure (PDB 2VCE) is superimposed onto the PGT
756 models to highlight the approximate position of the acceptor binding pocket.

757

758 **Figure 6. Engineering of Trilobatin and Phloridzin Production in *N. benthamiana*.**

759 *Nicotiana benthamiana* leaves were infiltrated with *Agrobacterium* suspensions containing
760 pHEX2_PGT2, pHEX2_PGT1 or the negative control pHEX2_GUS (each in combination
761 with pHEX2_MdMyb10, pHEX2_MdCHS, pHEX2_MdDBR + pBIN61-p19). Production of
762 trilobatin and phloridzin were analyzed by Dionex-HPLC 7 d post-infiltration. Experiments

763 were performed in triplicate and a single representative trace is shown. (A) pHEX2_PGT2; (B)
764 trilobatin [T] standard; (C) pHEX2_PGT1; (D) phloridzin [P] standard; (E) negative control
765 pHEX2_GUS.

766

767 **Figure 7. *PGT2* Expression Levels and Dihydrochalcone Content in Transgenic GL3**
768 **Apple Lines.**

769 (A) Relative expression of *PGT2* in fourteen transgenic GL3 lines (#) was determined by
770 RT-qPCR using RNA extracted from young leaves. Expression was corrected against
771 *MdACTIN* and is given relative to the wildtype (WT) GL3 control (value set at 1). Primers
772 and product sizes are given in Table S3. (B) Phenolic compounds were extracted from young
773 leaves and individual DHC content determined by HPLC. Data in panels A and B are
774 presented as mean \pm SE, n = 3 biological replicates. Statistical analysis was performed in
775 GraphPad Prism: one-way ANOVA using Dunnett's Multiple Comparison Test vs WT. No
776 significant differences in phloridzin or phloretin content were observed. Significantly higher
777 *PGT2* expression and trilobatin content vs control are shown at $P < 0.001 = ***$, $P < 0.01 = **$,
778 $P < 0.05 = *$, ns = not significant.

779

780 **Figure 8. Physiology of *PGT2* Transgenic Lines Grown Under Simulated Field**
781 **Conditions.**

782 (A) Phenotype at age 18 months of wildtype (WT) and three *PGT2* transgenic lines (#1, #5
783 and #14); (B) plant height, n = 3 trees per line; (C) the total number of branches per tree, n = 5
784 trees per line; (D) leaf phenotype; (E) fresh weight per leaf, n = 5 trees per line, 3 leaves per
785 tree; (F) powdery mildew infection phenotype in the young leaves of *PGT2* line #1; and (G)
786 powdery mildew infection rate, n = 5 trees per line, 3 leaves per tree. Data are presented as
787 mean \pm SE. Statistical analysis was performed in GraphPad Prism: one-way ANOVA using
788 Dunnett's Multiple Comparison Test vs WT. No significant differences in plant height, branch
789 number, leaf weight, or infection rate were observed.

790

791 **Figure 9. Analysis of Apple Leaf Teas and Trilobatin Iso-sweetness.**

792 (A) Phenolic compounds were extracted from dried leaf material and apple leaf tea prepared

793 from wildtype (WT) apple and two transgenic GL3 lines over-expressing *PGT2* (#1, #9).
794 Individual phloridzin (P) and trilobatin (T) content was determined by HPLC. Data are
795 presented as mean \pm SE, $n \geq 7$ for dried leaf material (DM) and $n = 3$ for apple leaf teas (LT).
796 Statistical analysis was performed in GraphPad Prism: one-way ANOVA using Dunnett's
797 Multiple Comparison Test vs WT. Significantly higher than WT at $P < 0.001 = ***$. (B)
798 Iso-sweetness comparison test between trilobatin and sucrose. Each participant was given one
799 trilobatin solution and eight sucrose solutions at different concentrations to taste.
800 Iso-sweetness was established as 35.2 ± 1.66 ($R^2 = 0.98$). Data presented are mean \pm SE, $n =$
801 5 participants.

802 **REFERENCES**

- 803 **Andre CM, Greenwood JM, Walker EG, Rassam M, Sullivan M, Evers D, Perry NB, Laing WA** (2012)
804 Anti-inflammatory procyanidins and triterpenes in 109 apple varieties. *J Agric Food Chem* **60**:
805 10546-10554
- 806 **Bray GA, Popkin BM** (2014) Dietary sugar and body weight: have we reached a crisis in the epidemic of obesity
807 and diabetes?: health be damned! Pour on the sugar. *Diabetes Care* **37**: 950-956
- 808 **Brazier-Hicks M, Offen W, Gershater M, Revett T, Lim E-K, Bowles D, Davies G, Edwards R** (2007)
809 Characterization and engineering of the bifunctional *N*- and *O*-glucosyltransferase involved in
810 xenobiotic metabolism in plants. *Proc Natl Acad Sci USA* **104**: 20238-20243
- 811 **Caputi L, Malnoy M, Goremykin V, Nikiforova S, Martens S** (2012) A genome-wide phylogenetic reconstruction
812 of family 1 UDP-glycosyltransferases revealed the expansion of the family during the adaptation of
813 plants to life on land. *Plant J* **69**: 1030-1042
- 814 **Chagné D, Crowhurst RN, Troggio M, Davey MW, Gilmore B, Lawley C, Vanderzande S, Hellens RP, Kumar S,
815 Cestaro A, et al.** (2012) Genome-wide SNP detection, validation, and development of an 8K SNP array
816 for apple. *PLoS One* **7**: e31745
- 817 **Chagné D, Gasic K, Crowhurst RN, Han Y, Bassett HC, Bowatte DR, Lawrence TJ, Rikkerink EH, Gardiner SE,
818 Korban SS** (2008) Development of a set of SNP markers present in expressed genes of the apple.
819 *Genomics* **92**: 353-358
- 820 **Daccord N, Celton JM, Linsmith G, Becker C, Choisne N, Schijlen E, van de Geest H, Bianco L, Micheletti D,
821 Velasco R, et al.** (2017) High-quality *de novo* assembly of the apple genome and methylome dynamics
822 of early fruit development. *Nat Genet*
- 823 **Dai H, Li W, Han G, Yang Y, Ma Y, Li H, Zhang Z** (2013) Development of a seedling clone with high regeneration
824 capacity and susceptibility to *Agrobacterium* in apple. *Sci Hortic* **164**: 202-208
- 825 **Dare AP, Tomes S, Cooney JM, Greenwood DR, Hellens RP** (2013a) The role of enoyl reductase genes in
826 phloridzin biosynthesis in apple. *Plant Physiol Biochem* **72**: 54-61
- 827 **Dare AP, Tomes S, Jones M, McGhie TK, Stevenson DE, Johnson RA, Greenwood DR, Hellens RP** (2013b)
828 Phenotypic changes associated with RNA interference silencing of chalcone synthase in apple (*Malus x*
829 *domestica*). *Plant J* **74**: 398-410
- 830 **Dare AP, Yauk Y-K, Tomes S, McGhie TK, Rebstock RS, Cooney JM, Atkinson RG** (2017) Silencing a
831 phloretin-specific glycosyltransferase perturbs both general phenylpropanoid biosynthesis and plant
832 development. *Plant J* **91**: 237-250
- 833 **Eichenberger M, Lehka BJ, Folly C, Fischer D, Martens S, Simon E, Naesby M** (2016) Metabolic engineering of
834 *Saccharomyces cerevisiae* for *de novo* production of dihydrochalcones with known antioxidant,
835 antidiabetic, and sweet tasting properties. *Metab Eng* **39**: 80-89
- 836 **Elejalde-Palmett C, Billet K, Lanoue A, De Craene JO, Glevarec G, Pichon O, Clastre M, Courdavault V,
837 St-Pierre B, Giglioli-Guivarc'h N, et al.** (2018) Genome-wide identification and biochemical
838 characterization of the UGT88F subfamily in *Malus x domestica* Borkh. *Phytochem* **157**: 135-144
- 839 **Espley RV, Hellens RP, Putterill J, Stevenson DE, Kutty-Amma S, Allan AC** (2007) Red colouration in apple fruit
840 is due to the activity of the MYB transcription factor, MdMYB10. *Plant J* **49**: 414-427
- 841 **Fan X, Zhang Y, Dong H, Wang B, Ji H, Liu X** (2015) Trilobatin attenuates the LPS-mediated inflammatory
842 response by suppressing the NF-kappaB signaling pathway. *Food Chem* **166**: 609-615
- 843 **Fukuchi-Mizutani M, Okuhara H, Fukui Y, Nakao M, Katsumoto Y, Yonekura-Sakakibara K, Kusumi T, Hase T,
844 Tanaka Y** (2003) Biochemical and molecular characterization of a novel UDP-glucose:anthocyanin
845 3'-*O*-glucosyltransferase, a key enzyme for blue anthocyanin biosynthesis, from gentian. *Plant Physiol*

- 846 **132**: 1652-1663
- 847 **Gao L, Li Z, Xia C, Qu Y, Liu M, Yang P, Yu L, Song X** (2017) Combining manipulation of transcription factors and
848 overexpression of the target genes to enhance lignocellulolytic enzyme production in *Penicillium*
849 *oxalicum*. *Biotechnol Biofuels* **10**: 100
- 850 **Gosch C, Flachowsky H, Halbwirth H, Thill J, Mjka-Wittmann R, Treutter D, Richter K, Hanke M-V, Stich K**
851 (2012) Substrate specificity and contribution of the glycosyltransferase UGT71A15 to phloridzin
852 biosynthesis. *Trees* **26**: 259-271
- 853 **Gosch C, Halbwirth H, Kuhn J, Miosic S, Stich K** (2009) Biosynthesis of phloridzin in apple (*Malus domestica*
854 Borkh.). *Plant Sci* **176**: 223-231
- 855 **Gosch C, Halbwirth H, Schneider B, Holscher D, Stich K** (2010) Cloning and heterologous expression of
856 glycosyltransferases from *Malus x domestica* and *Pyrus communis*, which convert phloretin to
857 phloretin 2'-O-glucoside (phloridzin). *Plant Sci* **178**: 299-306
- 858 **Gutierrez BL, Arro J, Zhong G-Y, Brown SK** (2018a) Linkage and association analysis of dihydrochalcones
859 phloridzin, sieboldin, and trilobatin in *Malus*. *Tree Genet Genomes* **14**
- 860 **Gutierrez BL, Zhong G-Y, Brown SK** (2018b) Genetic diversity of dihydrochalcone content in *Malus* germplasm.
861 *Genet Resour Crop Ev* **65**: 1485-1502
- 862 **Hellens RP, Allan AC, Friel EN, Bolitho K, Grafton K, Templeton MD, Karunairetnam S, Gleave AP, Laing WA**
863 (2005) Transient expression vectors for functional genomics, quantification of promoter activity and
864 RNA silencing in plants. *Plant Methods* **1**: 13
- 865 **Hsu YH, Tagami T, Matsunaga K, Okuyama M, Suzuki T, Noda N, Suzuki M, Shimura H** (2017) Functional
866 characterization of UDP-rhamnose-dependent rhamnosyltransferase involved in anthocyanin
867 modification, a key enzyme determining blue coloration in *Lobelia erinus*. *Plant J* **89**: 325-337
- 868 **Hutabarat OS, Flachowsky H, Regos I, Miosic S, Kaufmann C, Faramarzi S, Alam MZ, Gosch C, Peil A, Richter K,**
869 **et al.** (2016) Transgenic apple plants overexpressing the chalcone 3-hydroxylase gene of *Cosmos*
870 *sulphureus* show increased levels of 3-hydroxyphloridzin and reduced susceptibility to apple scab and
871 fire blight. *Planta* **243**: 1213-1224
- 872 **Ibdah M, Berim A, Martens S, Valderrama AL, Palmieri L, Lewinsohn E, Gang DR** (2014) Identification and
873 cloning of an NADPH-dependent hydroxycinnamoyl-CoA double bond reductase involved in
874 dihydrochalcone formation in *Malus x domestica* Borkh. *Phytochem* **107**: 24-31
- 875 **Jia ZM, Yang X, Hansen CA, Naman CB, Simons CT, Slack J, P., Gray K** (2008) Consumables. *In*, Vol
876 WO2008148239A1
- 877 **Jugd  H, Nguy D, I. M, Cooney JM, Atkinson RG** (2008) Isolation and characterization of a novel
878 glycosyltransferase that converts phloretin to phlorizin, a potent antioxidant in apple. *FEBS Journal*
879 **275**: 3804-3814
- 880 **Kim NC, Kinghorn AD** (2002) Highly sweet compounds of plant origin. *Arch Pharm Res* **25**: 725-746
- 881 **Kroger M, Meister K, Kava R** (2006) Low-calorie sweeteners and other sugar substitutes: A review of the safety
882 issues. *Compr Rev Food Sci F* **5**: 35-47
- 883 **Lei L, Huang B, Liu A, Lu Y-J, Zhou J-L, Zhang J, Wong W-L** (2018) Enzymatic production of natural sweetener
884 trilobatin from citrus flavanone naringin using immobilised α -L-rhamnosidase as the catalyst. *Int J*
885 *Food Sci Tech* **53**: 2097-2103
- 886 **Li P, Ma F, Cheng L** (2013) Primary and secondary metabolism in the sun-exposed peel and the shaded peel of
887 apple fruit. *Physiol Plant* **148**: 9-24
- 888 **Li Y, Baldauf S, Lim EK, Bowles DJ** (2001) Phylogenetic analysis of the UDP-glycosyltransferase multigene family
889 of *Arabidopsis thaliana*. *J Biol Chem* **276**: 4338-4343

- 890 **Linsmith G, Rombauts S, Montanari S, Deng CH, Celton J-M, Guérif P, Liu C, Lohaus R, Zurn JD, Cestaro A, et al.**
891 (2019) Pseudo-chromosome length genome assembly of a double haploid 'Bartlett' pear (*Pyrus*
892 *communis* L.). bioRxiv: 643916
- 893 **Livak KJ, Schmittgen TD** (2001) Analysis of relative gene expression data using real-time quantitative PCR and
894 the $2^{-\Delta\Delta CT}$ method. *Methods* **25**: 402-408
- 895 **Malnoy M, Reynoird JP, Mourgues F, Chevreau E, Simoneau P** (2001) A method for isolating total RNA from
896 pear leaves. *Plant Mol Biol Rep* **19**: 69a–69f
- 897 **Nieuwenhuizen NJ, Green SA, Chen X, Bailleul EJD, Matich AJ, Wang MY, Atkinson RG** (2013) Functional
898 genomics reveals that a compact terpene synthase gene family can account for terpene volatile
899 production in apple. *Plant Physiol* **161**: 787-804
- 900 **Ross J, Li Y, Lim E, Bowles DJ** (2001) Higher plant glycosyltransferases. *Genome Biol* **2**: 3004.3001-3004.3006
- 901 **Sun X, Wang P, Jia X, Huo L, Che R, Ma F** (2018) Improvement of drought tolerance by overexpressing
902 MdATG18a is mediated by modified antioxidant system and activated autophagy in transgenic apple.
903 *Plant Biotechnol J* **16**: 545-557
- 904 **Sun Y-S** (2015) A method of sweetening natural bulk separation trilobatin. *In*, Vol CN104974201B
- 905 **Sun Y-S, Zhang YW** (2015) Preparation of isolated natural sweetener trilobatin by crushing trilobatin, adding
906 alcohol, heating to reflux, separating, filtering, separating filter residue and filter liquor, separating
907 filter residue, and combining filtered liquors. *In*, Vol CN104974201A
- 908 **Sun Y, Li W, Liu Z** (2015) Preparative isolation, quantification and antioxidant activity of dihydrochalcones from
909 Sweet Tea (*Lithocarpus polystachyus* Rehd.). *J Chromatogr B Analyt Technol Biomed Life Sci* **1002**:
910 372-378
- 911 **Tanaka T, Tanaka O, Kohda H, Chou W-H, Chen F-H** (1983) Isolation of trilobatin, a sweet
912 dihydrochalcone-glucoside from leaves of *Vitis piasezkii* Maxim and *Vitis saccharifera* Makino. *Agric*
913 *Biol Chem* **47**: 2403-2404
- 914 **van Ooijen J** (2006) JoinMap® 4, Software for the calculation of genetic linkage maps in experimental
915 populations. *In* K B.V., ed, Wageningen, Netherlands
- 916 **Velasco R, Zharkikh A, Affourtit J, Dhingra A, Cestaro A, Kalyanaraman A, Fontana P, Bhatnagar SK, Troglio M,**
917 **Pruss D, et al.** (2010) The genome of the domesticated apple (*Malus x domestica* Borkh.). *Nat Genet*
918 **42**: 833-841
- 919 **Walton S, K., Denardo T, Zanno P, R., Topalovic M** (2015) Taste modifiers. *In*, Vol WO2013074811A1
- 920 **Williams AH** (1982) Chemical evidence from the flavonoids relevant to the classification of *Malus* species. *Bot J*
921 *Linn Soc* **84**: 31-39
- 922 **Xiao Z, Zhang Y, Chen X, Wang Y, Chen W, Xu Q, Li P, Ma F** (2017) Extraction, identification, and antioxidant and
923 anticancer tests of seven dihydrochalcones from *Malus* 'Red Splendor' fruit. *Food Chem* **231**: 324-331
- 924 **Yahyaa M, Ali S, Davidovich-Rikanati R, Ibdah M, Shachtier A, Eyal Y, Lewinsohn E, Ibdah M** (2017)
925 Characterization of three chalcone synthase-like genes from apple (*Malus x domestica* Borkh.).
926 *Phytochem* **140**: 125-133
- 927 **Yahyaa M, Davidovich-Rikanati R, Eyal Y, Sheachter A, Marzouk S, Lewinsohn E, Ibdah M** (2016) Identification
928 and characterization of UDP-glucose:phloretin 4'-O-glycosyltransferase from *Malus x domestica* Borkh.
929 *Phytochem* **130**: 47-55
- 930 **Yang J, Zhang Y** (2015) I-TASSER server: new development for protein structure and function predictions.
931 *Nucleic Acids Res* **43**: W174-W181
- 932 **Yao JL, Cohen D, Atkinson R, Richardson K, Morris B** (1995) Regeneration of transgenic plants from the
933 commercial apple cultivar Royal Gala. *Plant Cell Rep* **14**: 407-412

- 934 **Yao JL, Tomes S, Gleave AP** (2013) Transformation of apple (*Malus x domestica*) using mutants of apple
935 acetolactate synthase as a selectable marker and analysis of the T-DNA integration sites. *Plant Cell Rep*
936 **32**: 703-714
- 937 **Yauk Y-K, Ged C, Wang MY, Matich AJ, Tessarotto L, Cooney JM, Chervin C, Atkinson RG** (2014) Manipulation
938 of flavour and aroma compound sequestration and release using a glycosyltransferase with specificity
939 for terpene alcohols. *Plant J* **80**: 317-330
- 940 **Zhang L, Xu Q, You Y, Chen W, Xiao Z, Li P, Ma F** (2018) Characterization of quercetin and its glycoside
941 derivatives in *Malus* germplasm. *Hortic Environ Biotech* **59**: 909-917
- 942 **Zhou K, Hu L, Li P, Gong X, Ma F** (2017) Genome-wide identification of glycosyltransferases converting
943 phloretin to phloridzin in *Malus* species. *Plant Sci* **265**: 131-145
- 944 **Zhou K, Hu L, Li Y, Chen X, Zhang Z, Liu B, Li P, Gong X, Ma F** (2019) MdUGT88F1-mediated phloridzin
945 biosynthesis regulates apple development and *Valsa* canker resistance. *Plant Physiol* **180**: 2290-2305
- 946

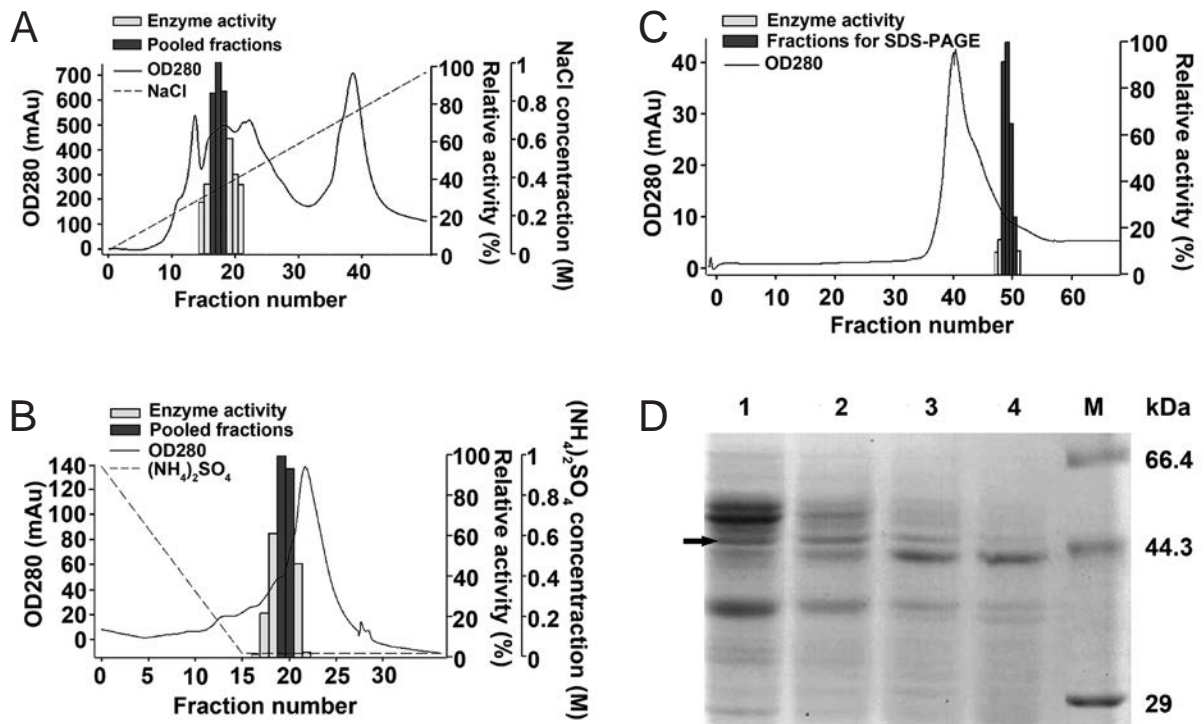


Figure 1. Activity-directed Purification of Ph4'-oGT Activity from Flowers of the Crabapple Hybrid 'Adams'.

Active fractions are shown as dark grey bars. (A) Purification by Q-sepharose chromatography. (B) Purification by phenyl sepharose chromatography using pooled fractions from Q-sepharose. (C) Purification by Superdex 75 chromatography using pooled fractions from phenyl sepharose. Protein concentration (280 nm), enzyme activity, pooled fractions and NaCl or $(\text{NH}_4)_2\text{SO}_4$ gradient in the elution buffer are indicated. (D) SDS-PAGE analysis of the four active fractions after purification by Superdex 75 chromatography are shown in lanes 1–4. M = Premixed Broad protein marker (Takara, Dalian, China). Arrow indicates the band sent for LC-MS/MS analysis.

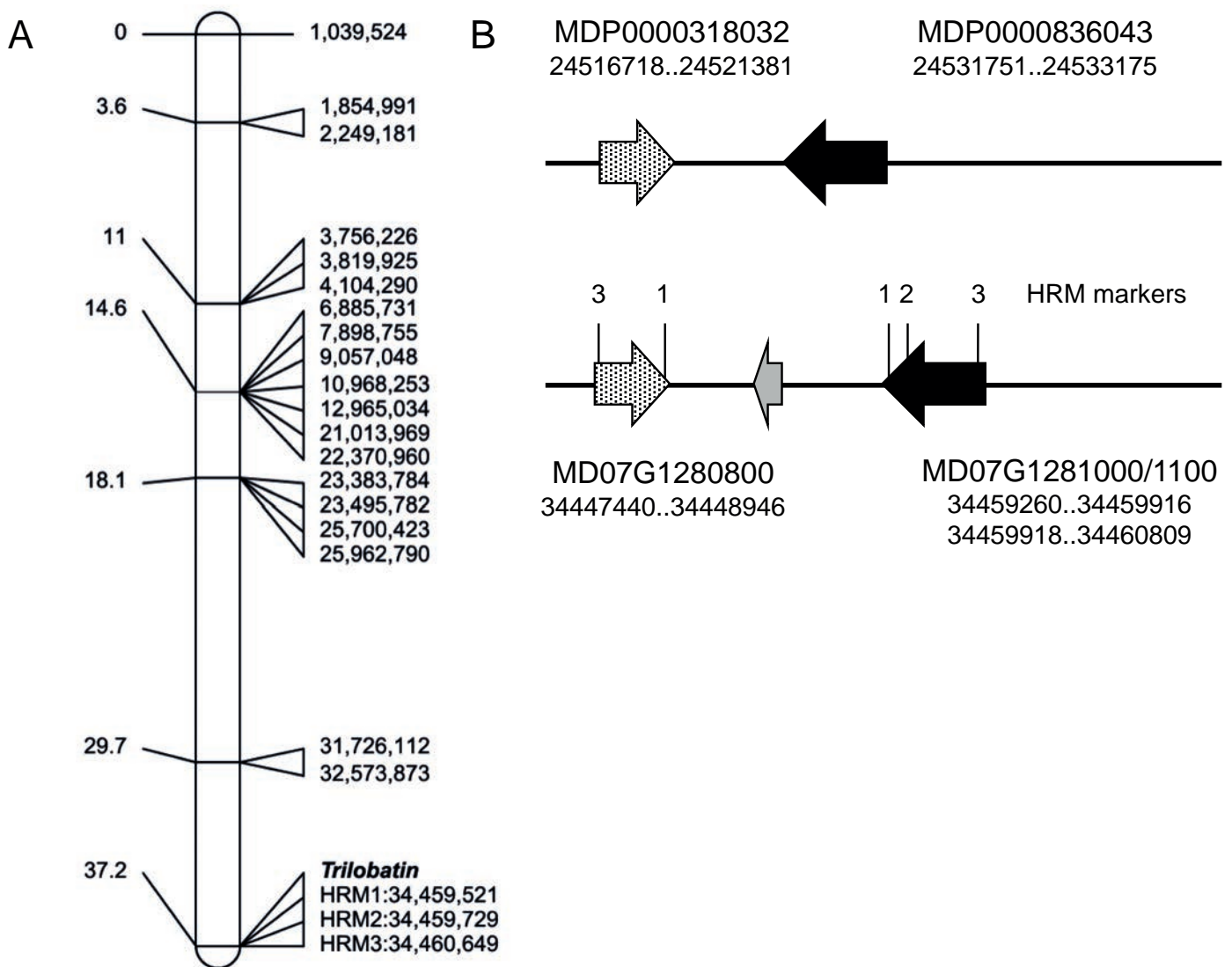


Figure 2. Genetic Mapping of Trilobatin production in a ‘Royal Gala’ x Y3 Segregating Population.

(A) The *Trilobatin* locus was mapped near the base of LG7 of Y3 using the IRSC 8K SNP array (Chagné et al., 2012). Genetic locations in centiMorgan (cM) are shown on the left and physical location in base pairs on the right (based on the ‘Golden Delicious’ doubled-haploid assembly GDDH13 v1.1). The physical locations of three HRM-SNP markers (Figure S1; Table S3) are indicated. (B) The genomic region of the *Trilobatin* locus in the ‘Golden Delicious’ v1.0p assembly (top) and the doubled-haploid assembly GDDH13 v1.1 (bottom). The physical positions of two UDP-glucosyltransferase genes identified at the locus in each assembly are shown below the gene model. The black arrow corresponds to *PGT2*, the speckled arrow to *PGT3* and the gray arrow to MD07G1280900 (annotated as a suppressor of auxin resistance). N.B. *PGT2* in the doubled-haploid assembly was incorrectly annotated as two truncated gene models MD07G1281000 and MD07G1281100. N.B. HRM1 and 3 amplified on both genes.

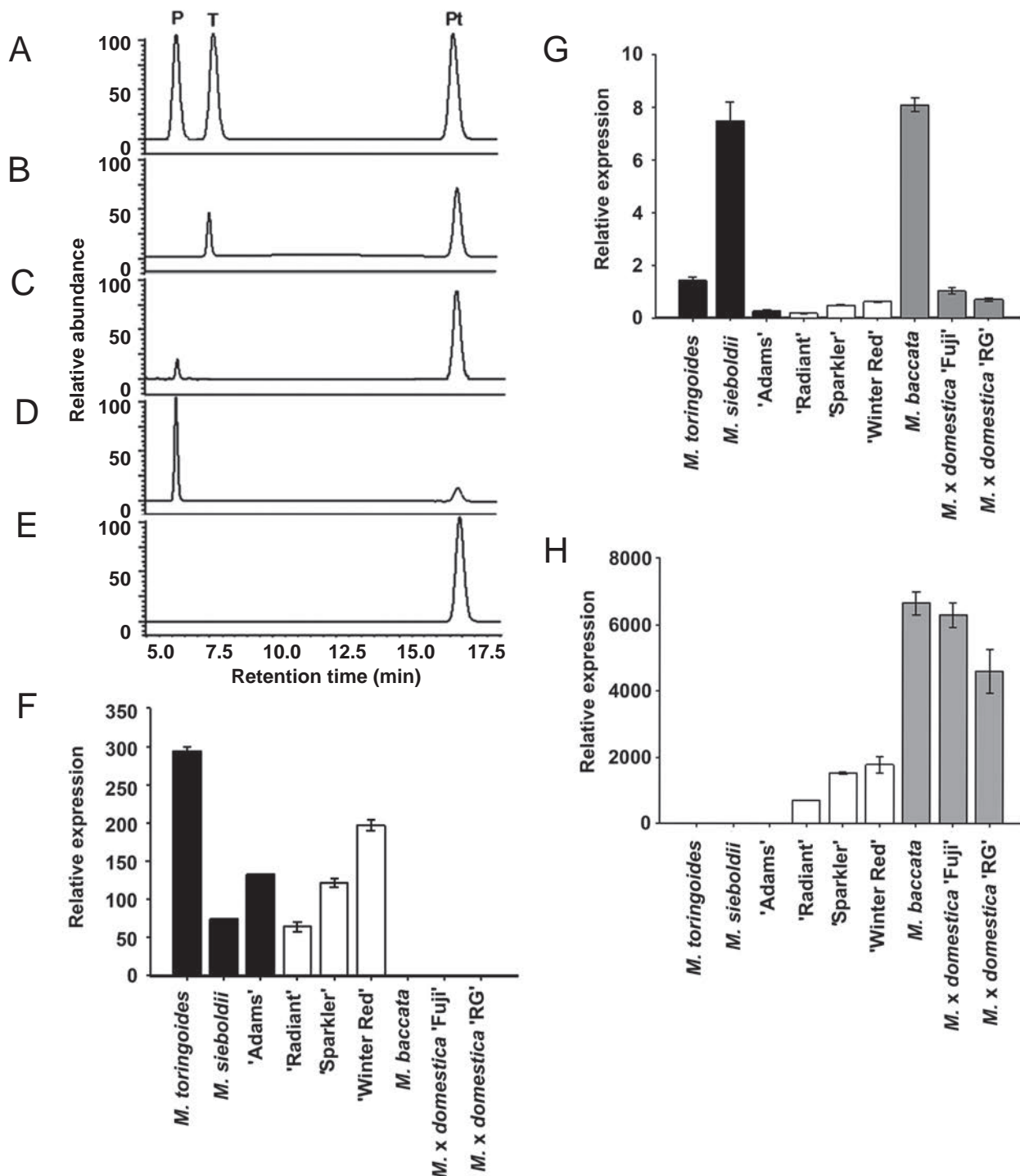


Figure 3. Biochemical and Expression Analysis of PGT1-3.

(A) Authentic standards of P = phloridzin, T = trilobatin and Pt = phloretin compared with the products formed by recombinant PGT2 from *M. toringoides* (B), PGT3 from *M. sieboldii* (C), PGT1 from *M. x domestica* 'Fuji' (D) and an empty vector control (E) in the presence phloretin and UDP-glucose. Experiments were performed in triplicate and a single representative trace is shown. Expression of PGT2 (F), PGT3 (G) and PGT1 (H) were analyzed by RT-qPCR using gene-specific primers (Table S3) in three *Malus* accessions containing only trilobatin (black bars), three containing trilobatin and phloridzin (white bars), and three containing only phloridzin (gray bars). *MdACTIN* was used as the reference gene. RG = 'Royal Gala'. Data are means (\pm SE) of three biological replicates from young leaves. Expression is presented relative to *M. x domestica* 'Fuji' in (F) and (G) and to *M. toringoides* in (H) (values set as 1).

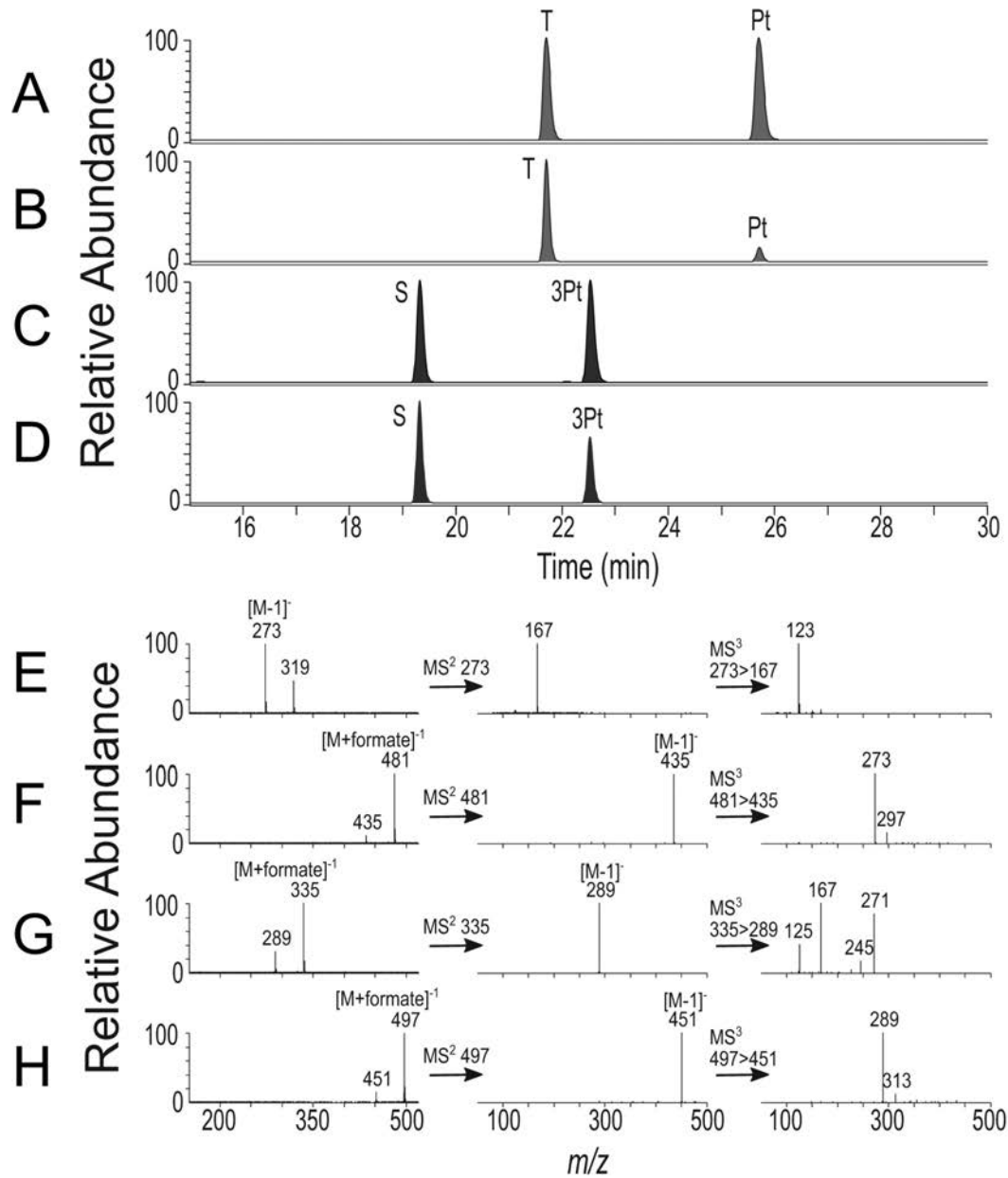


Figure 4. LC-MS/MS Analysis of Products Formed by *PGT2*.

Base peak plots: (A) mixed standard of phloretin (Pt) and trilobatin (T); (B) *PGT2* + phloretin + UDP-glucose; (C) mixed standard of 3-OH phloretin (3Pt) + sieboldin (S); (D) *PGT2* + 3-OH phloretin + UDP-glucose; Mass spectra for reaction products and standards: (E) fullscan, MS² and MS³ data for phloretin; (F) fullscan, MS² and MS³ data for trilobatin; (G) fullscan, MS² and MS³ data for 3-OH phloretin; and (H) fullscan, MS² and MS³ data for sieboldin.

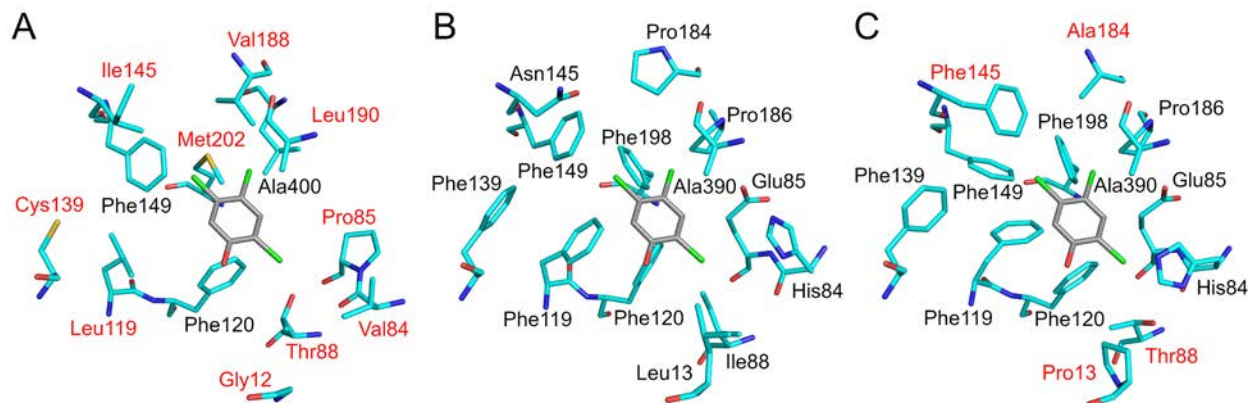


Figure 5. Structural Comparison of the Acceptor Binding Pockets of PGT1–PGT3 Models. The models were constructed by the iTASSER server. PGT1 (A) and PGT3 (C) residues labelled in red are different from PGT2 (B). The TCP (2,4,5-trichlorophenol) acceptor (shown in gray) from the UGT72B1 co-crystal structure (PDB 2VCE) is superimposed onto the PGT models to highlight the approximate position of the acceptor binding pocket.

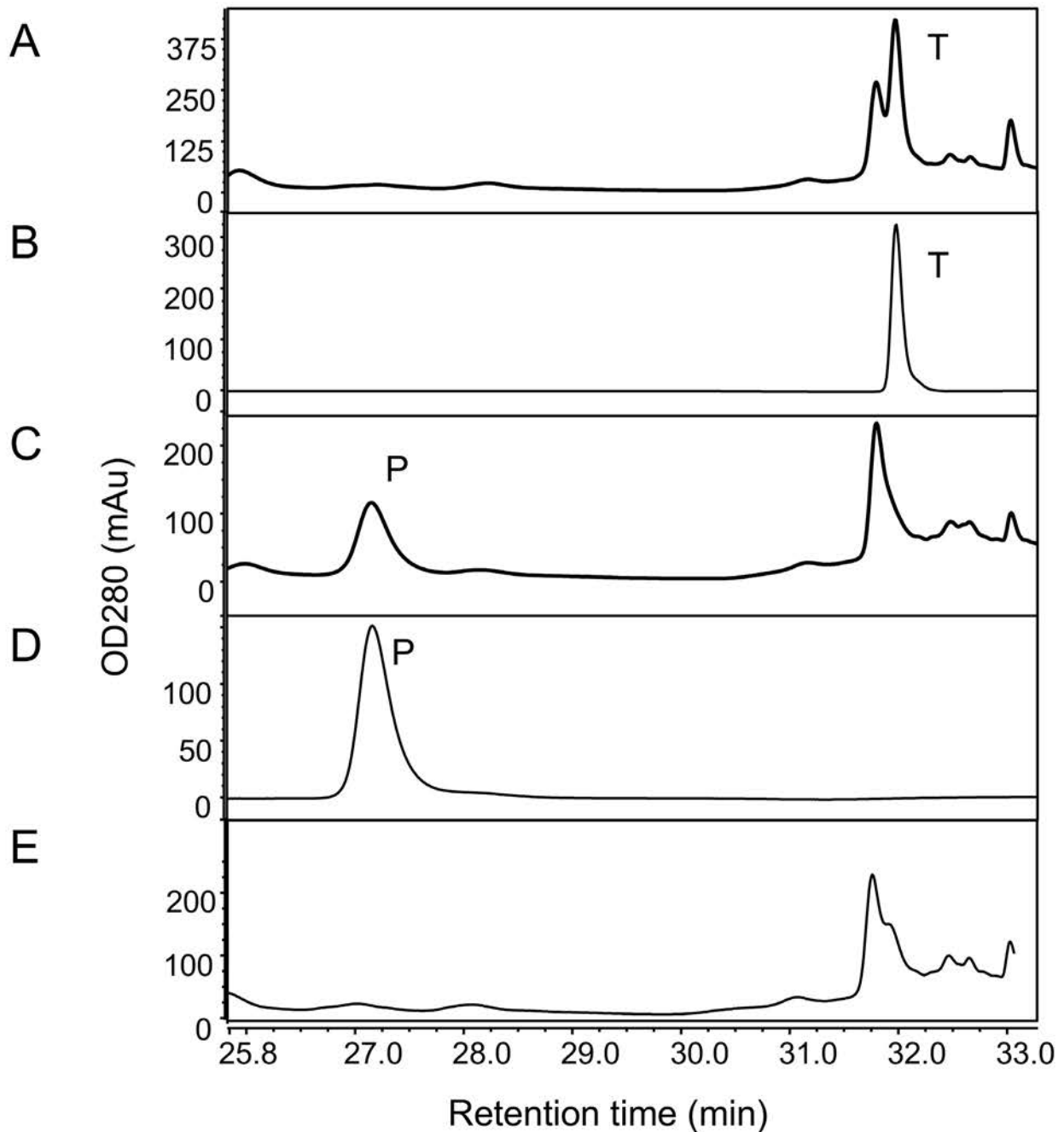


Figure 6. Engineering of Trilobatin and Phloridzin Production in Tobacco.

Nicotiana benthamiana leaves were infiltrated with *Agrobacterium* suspensions containing pHEX2_PGT2, pHEX2_PGT1 or the negative control pHEX2_GUS (each in combination with pHEX2_MdMyb10, pHEX2_MdCHS, pHEX2_MdDBR + pBIN61-p19). Production of trilobatin and phloridzin were analyzed by Dionex-HPLC 7 d post-infiltration. Experiments were performed in triplicate and a single representative trace is shown. (A) pHEX2_PGT2; (B) trilobatin [T] standard; (C) pHEX2_PGT1; (D) phloridzin [P] standard; (E) negative control pHEX2_GUS.

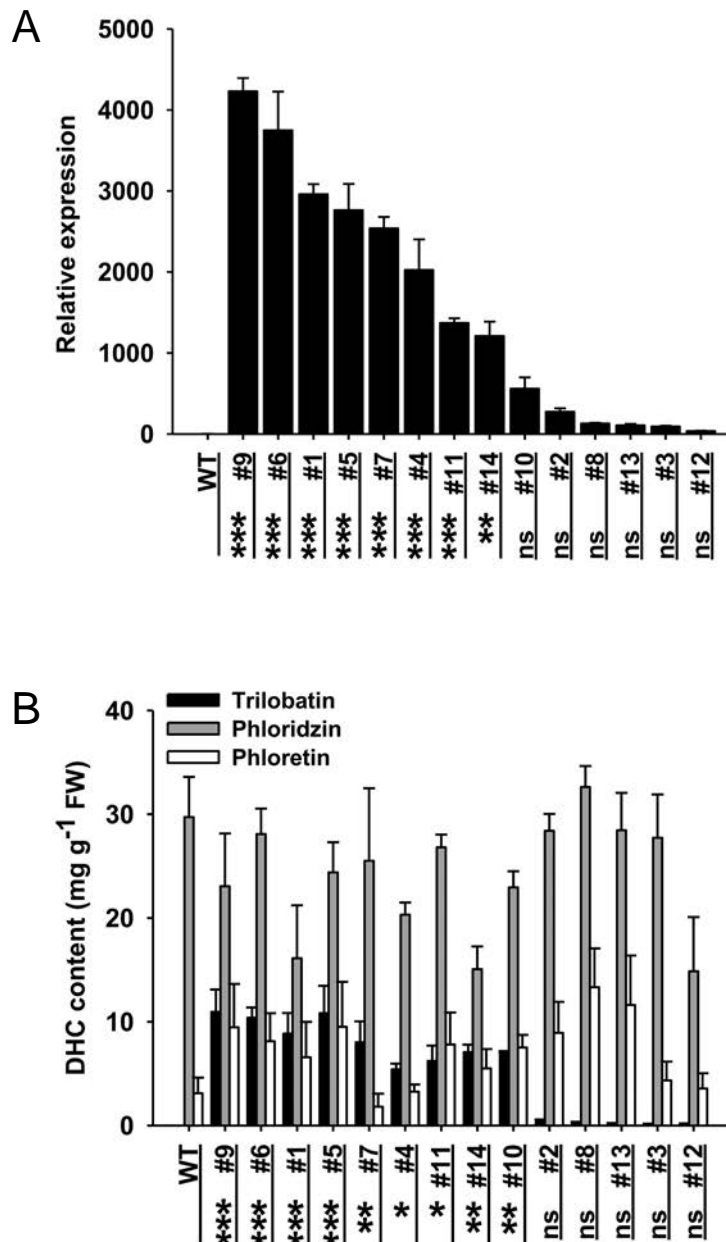


Figure 7. *PGT2* Expression Levels and Dihydrochalcone Content in Transgenic GL3 Apple Lines.

(A) Relative expression of *PGT2* in fourteen transgenic GL3 lines (#) was determined by RT-qPCR using RNA extracted from young leaves. Expression was corrected against *MdACTIN* and is given relative to the wildtype (WT) GL3 control (value set at 1). Primers and product sizes are given in Table S3. (B) Phenolic compounds were extracted from young leaves and individual DHC content determined by HPLC. Data in panels A and B are presented as mean \pm SE, $n = 3$ biological replicates. Statistical analysis was performed in GraphPad Prism: one-way ANOVA using Dunnett's Multiple Comparison Test vs WT. No significant differences in phloridzin or phloretin content were observed. Significantly higher *PGT2* expression and trilobatin content vs control are shown at $P < 0.001 = ***$, $P < 0.01 = **$, $P < 0.05 = *$, ns = not significant.

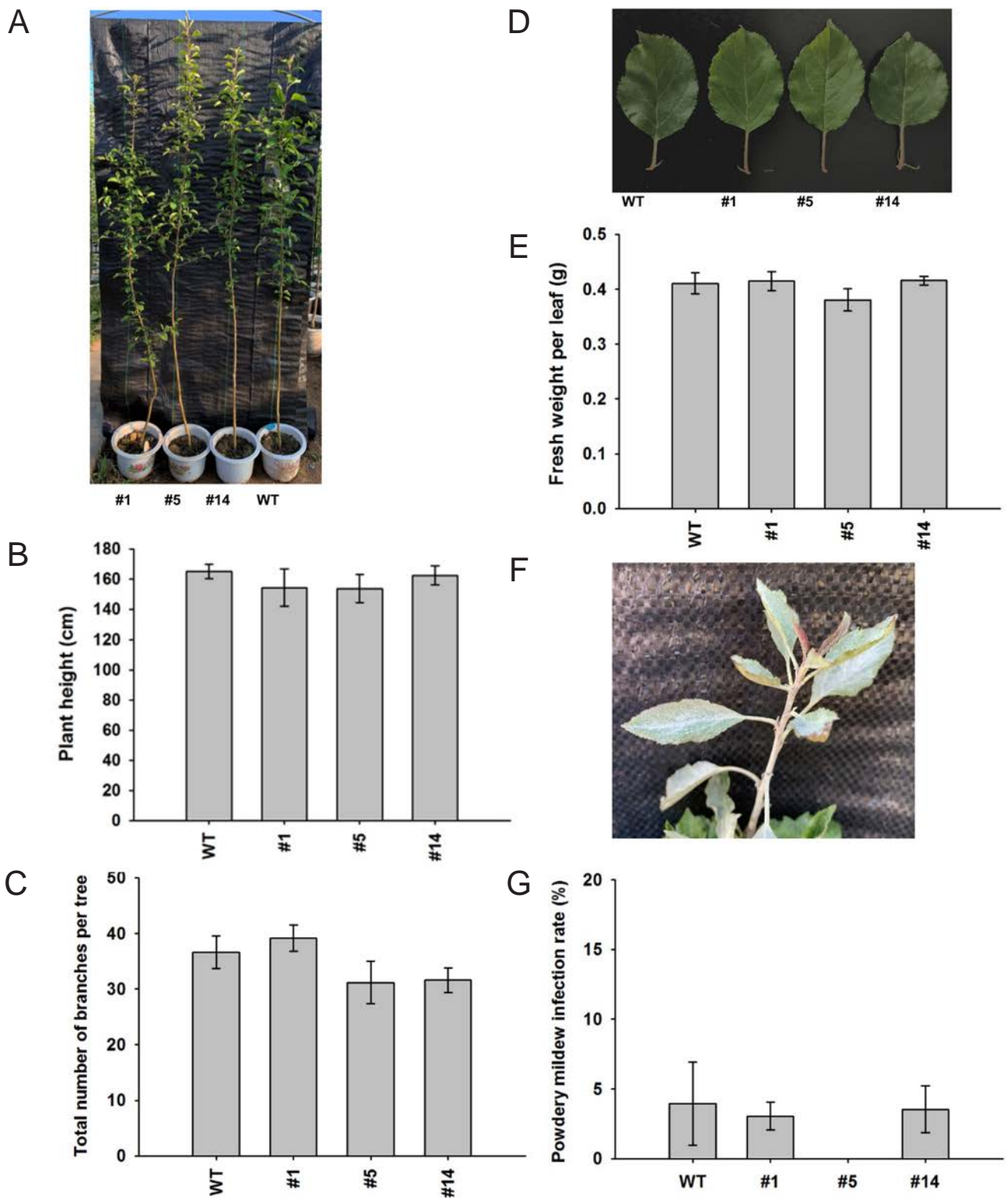


Figure 8. Physiology of *PGT2* Transgenic Lines Grown Under Simulated Field Conditions.

(A) Phenotype at age 18 months of wildtype (WT) and three *PGT2* transgenic lines (#1, #5 and #14); (B) plant height, $n = 3$ trees per line; (C) the total number of branches per tree, $n = 5$ trees per line; (D) leaf phenotype; (E) fresh weight per leaf, $n = 5$ trees per line, 3 leaves per tree; (F) powdery mildew infection phenotype in the young leaves of *PGT2* line #1; and (G) powdery mildew infection rate, $n = 5$ trees per line, 3 leaves per tree. Data are presented as mean \pm SE. Statistical analysis was performed in GraphPad Prism: one-way ANOVA using Dunnett's Multiple Comparison Test vs WT. No significant differences in plant height, branch number, leaf weight, or infection rate were observed.

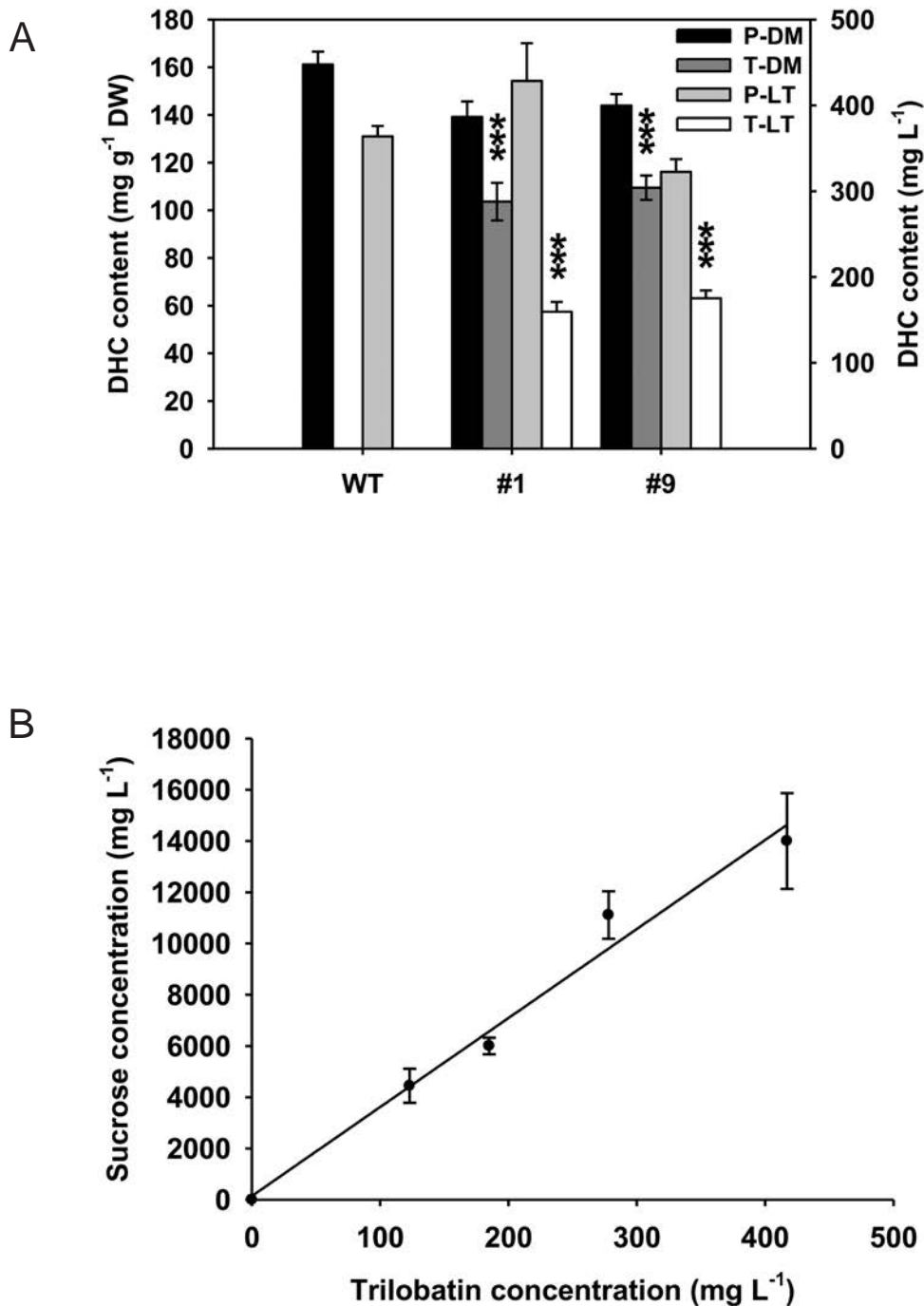


Figure 9. Analysis of Apple Leaf Teas and Trilobatin Iso-sweetness.

(A) Phenolic compounds were extracted from dried leaf material and apple leaf tea prepared from wildtype (WT) apple and two transgenic GL3 lines over-expressing *PGT2* (#1, #9). Individual phloridzin (P) and trilobatin (T) content was determined by HPLC. Data are presented as mean \pm SE, $n \geq 7$ for dried leaf material (DM) and $n = 3$ for apple leaf teas (LT). Statistical analysis was performed in GraphPad Prism: one-way ANOVA using Dunnett's Multiple Comparison Test vs WT. Significantly higher than WT at $P < 0.001 = ***$. (B) Iso-sweetness comparison test between trilobatin and sucrose. Each participant was given one trilobatin solution and eight sucrose solutions at different concentrations to taste. Iso-sweetness was established as 35.2 ± 1.66 ($R^2 = 0.98$). Data presented are mean \pm SE, $n = 5$ participants.

Parsed Citations

Andre CM, Greenwood JM, Walker EG, Rassam M, Sullivan M, Evers D, Perry NB, Laing WA (2012) Anti-inflammatory procyanidins and triterpenes in 109 apple varieties. J Agric Food Chem 60: 10546-10554

Pubmed: [Author and Title](#)

Google Scholar: [Author Only Title Only Author and Title](#)

Bray GA, Popkin BM (2014) Dietary sugar and body weight: have we reached a crisis in the epidemic of obesity and diabetes?: health be damned! Pour on the sugar. Diabetes Care 37: 950-956

Pubmed: [Author and Title](#)

Google Scholar: [Author Only Title Only Author and Title](#)

Brazier-Hicks M, Offen W, Gershater M, Revett T, Lim E-K, Bowles D, Davies G, Edwards R (2007) Characterization and engineering of the bifunctional N- and O-glucosyltransferase involved in xenobiotic metabolism in plants. Proc Natl Acad Sci USA 104: 20238-20243

Pubmed: [Author and Title](#)

Google Scholar: [Author Only Title Only Author and Title](#)

Caputi L, Malnoy M, Goremykin V, Nikiforova S, Martens S (2012) A genome-wide phylogenetic reconstruction of family 1 UDP-glycosyltransferases revealed the expansion of the family during the adaptation of plants to life on land. Plant J 69: 1030-1042

Pubmed: [Author and Title](#)

Google Scholar: [Author Only Title Only Author and Title](#)

Chagné D, Crowhurst RN, Troggio M, Davey MW, Gilmore B, Lawley C, Vanderzande S, Hellens RP, Kumar S, Cestaro A, et al. (2012) Genome-wide SNP detection, validation, and development of an 8K SNP array for apple. PloS One 7: e31745

Pubmed: [Author and Title](#)

Google Scholar: [Author Only Title Only Author and Title](#)

Chagné D, Gasic K, Crowhurst RN, Han Y, Bassett HC, Bowatte DR, Lawrence TJ, Rikkerink EH, Gardiner SE, Korban SS (2008) Development of a set of SNP markers present in expressed genes of the apple. Genomics 92: 353-358

Pubmed: [Author and Title](#)

Google Scholar: [Author Only Title Only Author and Title](#)

Daccord N, Celton JM, Linsmith G, Becker C, Choisine N, Schijlen E, van de Geest H, Bianco L, Micheletti D, Velasco R, et al. (2017) High-quality de novo assembly of the apple genome and methylome dynamics of early fruit development. Nat Genet

Pubmed: [Author and Title](#)

Google Scholar: [Author Only Title Only Author and Title](#)

Dai H, Li W, Han G, Yang Y, Ma Y, Li H, Zhang Z (2013) Development of a seedling clone with high regeneration capacity and susceptibility to *Agrobacterium* in apple. Sci Hortic 164: 202-208

Pubmed: [Author and Title](#)

Google Scholar: [Author Only Title Only Author and Title](#)

Dare AP, Tomes S, Cooney JM, Greenwood DR, Hellens RP (2013a) The role of enoyl reductase genes in phloridzin biosynthesis in apple. Plant Physiol Biochem 72: 54-61

Pubmed: [Author and Title](#)

Google Scholar: [Author Only Title Only Author and Title](#)

Dare AP, Tomes S, Jones M, McGhie TK, Stevenson DE, Johnson RA, Greenwood DR, Hellens RP (2013b) Phenotypic changes associated with RNA interference silencing of chalcone synthase in apple (*Malus x domestica*). Plant J 74: 398-410

Pubmed: [Author and Title](#)

Google Scholar: [Author Only Title Only Author and Title](#)

Dare AP, Yauk Y-K, Tomes S, McGhie TK, Rebstock RS, Cooney JM, Atkinson RG (2017) Silencing a phloretin-specific glycosyltransferase perturbs both general phenylpropanoid biosynthesis and plant development. Plant J 91: 237-250

Pubmed: [Author and Title](#)

Google Scholar: [Author Only Title Only Author and Title](#)

Eichenberger M, Lehka BJ, Folly C, Fischer D, Martens S, Simon E, Naesby M (2016) Metabolic engineering of *Saccharomyces cerevisiae* for de novo production of dihydrochalcones with known antioxidant, antidiabetic, and sweet tasting properties. Metab Eng 39: 80-89

Pubmed: [Author and Title](#)

Google Scholar: [Author Only Title Only Author and Title](#)

Elejalde-Palmett C, Billet K, Lanoue A, De Craene JO, Glevarec G, Pichon O, Clastre M, Courdavault V, St-Pierre B, Giglioli-Guivarc'h N, et al. (2018) Genome-wide identification and biochemical characterization of the UGT88F subfamily in *Malus x domestica* Borkh. Phytochem 157: 135-144

Pubmed: [Author and Title](#)

Google Scholar: [Author Only Title Only Author and Title](#)

Espley RV, Hellens RP, Putterill J, Stevenson DE, Kutty-Amma S, Allan AC (2007) Red colouration in apple fruit is due to the activity of the MYB transcription factor, MdMYB10. Plant J 49: 414-427

Pubmed: [Author and Title](#)

Google Scholar: [Author Only Title Only Author and Title](#)

Fan X, Zhang Y, Dong H, Wang B, Ji H, Liu X (2015) Trilobatin attenuates the LPS-mediated inflammatory response by suppressing the NF-kappaB signaling pathway. *Food Chem* 166: 609-615

Pubmed: [Author and Title](#)

Google Scholar: [Author Only](#) [Title Only](#) [Author and Title](#)

Fukuchi-Mizutani M, Okuhara H, Fukui Y, Nakao M, Katsumoto Y, Yonekura-Sakakibara K, Kusumi T, Hase T, Tanaka Y (2003) Biochemical and molecular characterization of a novel UDP-glucose:anthocyanin 3'-O-glucosyltransferase, a key enzyme for blue anthocyanin biosynthesis, from gentian. *Plant Physiol* 132: 1652-1663

Pubmed: [Author and Title](#)

Google Scholar: [Author Only](#) [Title Only](#) [Author and Title](#)

Gao L, Li Z, Xia C, Qu Y, Liu M, Yang P, Yu L, Song X (2017) Combining manipulation of transcription factors and overexpression of the target genes to enhance lignocellulolytic enzyme production in *Penicillium oxalicum*. *Biotechnol Biofuels* 10: 100

Pubmed: [Author and Title](#)

Google Scholar: [Author Only](#) [Title Only](#) [Author and Title](#)

Gosch C, Flachowsky H, Halbwirth H, Thill J, Mjka-Wittmann R, Treutter D, Richter K, Hanke M-V, Stich K (2012) Substrate specificity and contribution of the glycosyltransferase UGT71A15 to phloridzin biosynthesis. *Trees* 26: 259-271

Pubmed: [Author and Title](#)

Google Scholar: [Author Only](#) [Title Only](#) [Author and Title](#)

Gosch C, Halbwirth H, Kuhn J, Miosic S, Stich K (2009) Biosynthesis of phloridzin in apple (*Malus domestica* Borkh.). *Plant Sci* 176: 223-231

Pubmed: [Author and Title](#)

Google Scholar: [Author Only](#) [Title Only](#) [Author and Title](#)

Gosch C, Halbwirth H, Schneider B, Holscher D, Stich K (2010) Cloning and heterologous expression of glycosyltransferases from *Malus x domestica* and *Pyrus communis*, which convert phloretin to phloretin 2'-O-glucoside (phloridzin). *Plant Sci* 178: 299-306

Pubmed: [Author and Title](#)

Google Scholar: [Author Only](#) [Title Only](#) [Author and Title](#)

Gutierrez BL, Arro J, Zhong G-Y, Brown SK (2018a) Linkage and association analysis of dihydrochalcones phloridzin, sieboldin, and trilobatin in *Malus*. *Tree Genet Genomes* 14

Pubmed: [Author and Title](#)

Google Scholar: [Author Only](#) [Title Only](#) [Author and Title](#)

Gutierrez BL, Zhong G-Y, Brown SK (2018b) Genetic diversity of dihydrochalcone content in *Malus* germplasm. *Genet Resour Crop Ev* 65: 1485-1502

Pubmed: [Author and Title](#)

Google Scholar: [Author Only](#) [Title Only](#) [Author and Title](#)

Hellens RP, Allan AC, Friel EN, Bolitho K, Grafton K, Templeton MD, Karunairetnam S, Gleave AP, Laing WA (2005) Transient expression vectors for functional genomics, quantification of promoter activity and RNA silencing in plants. *Plant Methods* 1: 13

Pubmed: [Author and Title](#)

Google Scholar: [Author Only](#) [Title Only](#) [Author and Title](#)

Hsu YH, Tagami T, Matsunaga K, Okuyama M, Suzuki T, Noda N, Suzuki M, Shimura H (2017) Functional characterization of UDP-rhamnose-dependent rhamnosyltransferase involved in anthocyanin modification, a key enzyme determining blue coloration in *Lobelia erinus*. *Plant J* 89: 325-337

Pubmed: [Author and Title](#)

Google Scholar: [Author Only](#) [Title Only](#) [Author and Title](#)

Hutabarat OS, Flachowsky H, Regos I, Miosic S, Kaufmann C, Faramarzi S, Alam MZ, Gosch C, Peil A, Richter K, et al. (2016) Transgenic apple plants overexpressing the chalcone 3-hydroxylase gene of *Cosmos sulphureus* show increased levels of 3-hydroxyphloridzin and reduced susceptibility to apple scab and fire blight. *Planta* 243: 1213-1224

Pubmed: [Author and Title](#)

Google Scholar: [Author Only](#) [Title Only](#) [Author and Title](#)

Ibdah M, Berim A, Martens S, Valderrama AL, Palmieri L, Lewinsohn E, Gang DR (2014) Identification and cloning of an NADPH-dependent hydroxycinnamoyl-CoA double bond reductase involved in dihydrochalcone formation in *Malus x domestica* Borkh. *Phytochem* 107: 24-31

Pubmed: [Author and Title](#)

Google Scholar: [Author Only](#) [Title Only](#) [Author and Title](#)

Jia ZM, Yang X, Hansen CA, Naman CB, Simons CT, Slack J, P., Gray K (2008) Consumables. In, Vol WO2008148239A1

Pubmed: [Author and Title](#)

Google Scholar: [Author Only](#) [Title Only](#) [Author and Title](#)

Jugd  H, Nguy D, I. M, Cooney JM, Atkinson RG (2008) Isolation and characterization of a novel glycosyltransferase that converts phloretin to phlorizin, a potent antioxidant in apple. *FEBS Journal* 275: 3804-3814

Pubmed: [Author and Title](#)

Google Scholar: [Author Only](#) [Title Only](#) [Author and Title](#)

Kim NC, Kinghorn AD (2002) Highly sweet compounds of plant origin. *Arch Pharm Res* 25: 725-746

- Pubmed: [Author and Title](#)
Google Scholar: [Author Only Title Only Author and Title](#)
- Kroger M, Meister K, Kava R (2006) Low-calorie sweeteners and other sugar substitutes: A review of the safety issues. *Compr Rev Food Sci F* 5: 35-47**
Pubmed: [Author and Title](#)
Google Scholar: [Author Only Title Only Author and Title](#)
- Lei L, Huang B, Liu A, Lu Y-J, Zhou J-L, Zhang J, Wong W-L (2018) Enzymatic production of natural sweetener trilobatin from citrus flavanone naringin using immobilised α -L-rhamnosidase as the catalyst. *Int J Food Sci Tech* 53: 2097-2103**
Pubmed: [Author and Title](#)
Google Scholar: [Author Only Title Only Author and Title](#)
- Li P, Ma F, Cheng L (2013) Primary and secondary metabolism in the sun-exposed peel and the shaded peel of apple fruit. *Physiol Plant* 148: 9-24**
Pubmed: [Author and Title](#)
Google Scholar: [Author Only Title Only Author and Title](#)
- Li Y, Baldauf S, Lim EK, Bowles DJ (2001) Phylogenetic analysis of the UDP-glycosyltransferase multigene family of *Arabidopsis thaliana*. *J Biol Chem* 276: 4338-4343**
Pubmed: [Author and Title](#)
Google Scholar: [Author Only Title Only Author and Title](#)
- Linsmith G, Rombauts S, Montanari S, Deng CH, Celton J-M, Guérif P, Liu C, Lohaus R, Zurn JD, Cestaro A, et al. (2019) Pseudo-chromosome length genome assembly of a double haploid 'Bartlett' pear (*Pyrus communis* L.). *bioRxiv*: 643916**
Pubmed: [Author and Title](#)
Google Scholar: [Author Only Title Only Author and Title](#)
- Livak KJ, Schmittgen TD (2001) Analysis of relative gene expression data using real-time quantitative PCR and the 2- $\Delta\Delta$ CT method. *Methods* 25: 402-408**
Pubmed: [Author and Title](#)
Google Scholar: [Author Only Title Only Author and Title](#)
- Malnoy M, Reynold JP, Mourgues F, Chevreau E, Simoneau P (2001) A method for isolating total RNA from pear leaves. *Plant Mol Biol Rep* 19: 69a-69f**
Pubmed: [Author and Title](#)
Google Scholar: [Author Only Title Only Author and Title](#)
- Nieuwenhuizen NJ, Green SA, Chen X, Bailleul EJD, Matich AJ, Wang MY, Atkinson RG (2013) Functional genomics reveals that a compact terpene synthase gene family can account for terpene volatile production in apple. *Plant Physiol* 161: 787-804**
Pubmed: [Author and Title](#)
Google Scholar: [Author Only Title Only Author and Title](#)
- Ross J, Li Y, Lim E, Bowles DJ (2001) Higher plant glycosyltransferases. *Genome Biol* 2: 3004.3001-3004.3006**
Pubmed: [Author and Title](#)
Google Scholar: [Author Only Title Only Author and Title](#)
- Sun X, Wang P, Jia X, Huo L, Che R, Ma F (2018) Improvement of drought tolerance by overexpressing MdATG18a is mediated by modified antioxidant system and activated autophagy in transgenic apple. *Plant Biotechnol J* 16: 545-557**
Pubmed: [Author and Title](#)
Google Scholar: [Author Only Title Only Author and Title](#)
- Sun Y-S (2015) A method of sweetening natural bulk separation trilobatin. In, Vol CN104974201B**
Pubmed: [Author and Title](#)
Google Scholar: [Author Only Title Only Author and Title](#)
- Sun Y-S, Zhang YW (2015) Preparation of isolated natural sweetener trilobatin by crushing trilobatin, adding alcohol, heating to reflux, separating, filtering, separating filter residue and filter liquor, separating filter residue, and combining filtered liquors. In, Vol CN104974201A**
Pubmed: [Author and Title](#)
Google Scholar: [Author Only Title Only Author and Title](#)
- Sun Y, Li W, Liu Z (2015) Preparative isolation, quantification and antioxidant activity of dihydrochalcones from Sweet Tea (*Lithocarpus polystachyus* Rehd.). *J Chromatogr B Analyt Technol Biomed Life Sci* 1002: 372-378**
Pubmed: [Author and Title](#)
Google Scholar: [Author Only Title Only Author and Title](#)
- Tanaka T, Tanaka O, Kohda H, Chou W-H, Chen F-H (1983) Isolation of trilobatin, a sweet dihydrochalcone-glucoside from leaves of *Vitis piasezkii* Maxim and *Vitis saccharifera* Makino. *Agric Biol Chem* 47: 2403-2404**
Pubmed: [Author and Title](#)
Google Scholar: [Author Only Title Only Author and Title](#)
- van Ooijen J (2006) JoinMap® 4, Software for the calculation of genetic linkage maps in experimental populations. In K B.V., ed, Wageningen, Netherlands**
Pubmed: [Author and Title](#)

Google Scholar: [Author Only](#) [Title Only](#) [Author and Title](#)

Velasco R, Zharkikh A, Affourtit J, Dhingra A, Cestaro A, Kalyanaraman A, Fontana P, Bhatnagar SK, Troglio M, Pruss D, et al. (2010) The genome of the domesticated apple (*Malus x domestica* Borkh.). *Nat Genet* 42: 833-841

Pubmed: [Author and Title](#)

Google Scholar: [Author Only](#) [Title Only](#) [Author and Title](#)

Walton S, K., Denardo T, Zanno P, R., Topalovic M (2015) Taste modifiers. In, Vol WO2013074811A1

Pubmed: [Author and Title](#)

Google Scholar: [Author Only](#) [Title Only](#) [Author and Title](#)

Williams AH (1982) Chemical evidence from the flavonoids relevant to the classification of *Malus* species. *Bot J Linn Soc* 84: 31-39

Pubmed: [Author and Title](#)

Google Scholar: [Author Only](#) [Title Only](#) [Author and Title](#)

Xiao Z, Zhang Y, Chen X, Wang Y, Chen W, Xu Q, Li P, Ma F (2017) Extraction, identification, and antioxidant and anticancer tests of seven dihydrochalcones from *Malus* 'Red Splendor' fruit. *Food Chem* 231: 324-331

Pubmed: [Author and Title](#)

Google Scholar: [Author Only](#) [Title Only](#) [Author and Title](#)

Yahya M, Ali S, Davidovich-Rikanati R, Ibdah M, Shachtier A, Eyal Y, Lewinsohn E, Ibdah M (2017) Characterization of three chalcone synthase-like genes from apple (*Malus x domestica* Borkh.). *Phytochem* 140: 125-133

Pubmed: [Author and Title](#)

Google Scholar: [Author Only](#) [Title Only](#) [Author and Title](#)

Yahya M, Davidovich-Rikanati R, Eyal Y, Sheachter A, Marzouk S, Lewinsohn E, Ibdah M (2016) Identification and characterization of UDP-glucose:phloretin 4'-O-glycosyltransferase from *Malus x domestica* Borkh. *Phytochem* 130: 47-55

Pubmed: [Author and Title](#)

Google Scholar: [Author Only](#) [Title Only](#) [Author and Title](#)

Yang J, Zhang Y (2015) I-TASSER server: new development for protein structure and function predictions. *Nucleic Acids Res* 43: W174-W181

Pubmed: [Author and Title](#)

Google Scholar: [Author Only](#) [Title Only](#) [Author and Title](#)

Yao JL, Cohen D, Atkinson R, Richardson K, Morris B (1995) Regeneration of transgenic plants from the commercial apple cultivar Royal Gala. *Plant Cell Rep* 14: 407-412

Pubmed: [Author and Title](#)

Google Scholar: [Author Only](#) [Title Only](#) [Author and Title](#)

Yao JL, Tomes S, Gleave AP (2013) Transformation of apple (*Malus x domestica*) using mutants of apple acetolactate synthase as a selectable marker and analysis of the T-DNA integration sites. *Plant Cell Rep* 32: 703-714

Pubmed: [Author and Title](#)

Google Scholar: [Author Only](#) [Title Only](#) [Author and Title](#)

Yauk Y-K, Ged C, Wang MY, Matich AJ, Tessarotto L, Cooney JM, Chervin C, Atkinson RG (2014) Manipulation of flavour and aroma compound sequestration and release using a glycosyltransferase with specificity for terpene alcohols. *Plant J* 80: 317-330

Pubmed: [Author and Title](#)

Google Scholar: [Author Only](#) [Title Only](#) [Author and Title](#)

Zhang L, Xu Q, You Y, Chen W, Xiao Z, Li P, Ma F (2018) Characterization of quercetin and its glycoside derivatives in *Malus* germplasm. *Hortic Environ Biotech* 59: 909-917

Pubmed: [Author and Title](#)

Google Scholar: [Author Only](#) [Title Only](#) [Author and Title](#)

Zhou K, Hu L, Li P, Gong X, Ma F (2017) Genome-wide identification of glycosyltransferases converting phloretin to phloridzin in *Malus* species. *Plant Sci* 265: 131-145

Pubmed: [Author and Title](#)

Google Scholar: [Author Only](#) [Title Only](#) [Author and Title](#)

Zhou K, Hu L, Li Y, Chen X, Zhang Z, Liu B, Li P, Gong X, Ma F (2019) MdUGT88F1-mediated phloridzin biosynthesis regulates apple development and Valsa canker resistance. *Plant Physiol* 180: 2290-2305

Pubmed: [Author and Title](#)

Google Scholar: [Author Only](#) [Title Only](#) [Author and Title](#)